Title
Imaging cell morphology and physiology using X-rays.

Journal
Biochemical Society Transactions, 47(2)

ISSN
0300-5127

Authors
Weinhardt, Venera
Chen, Jian-Hua
Ekman, Axel
et al.

Publication Date
2019-04-30

DOI
10.1042/bst20180036

Peer reviewed

Published in final edited form as:

Biochem Soc Trans. 2019 April 30; 47(2): 489–508. doi:10.1042/BST20180036.

Imaging Cell Morphology and Physiology using X-rays

Venera Weinhardt[1,2], **Jian-Hua Chen**[1], **Axel Ekman**[1], **Gerry McDermott**[1], **Mark A. Le Gros**[1,2], **Carolyn Larabell**[1,2]

[1]Molecular Biophysics and Integrated Bioimaging Division, Lawrence Berkeley National Laboratory, Berkeley, California, USA

[2]Department of Anatomy, University of California San Francisco, San Francisco, California, USA

Abstract

Morphometric measurements, such as quantifying cell shape, characterizing sub-cellular organization, and probing cell-cell interactions, are fundamental in cell biology and clinical medicine. Until quite recently, the main source of morphometric data on cells has been light- and electron-based microscope images. However, a number of technological advances have propelled X-ray microscopy into becoming another source of high-quality morphometric information. Here we review the status of X-ray microscopy as a quantitative biological imaging modality. We also describe the combination of X-ray microscopy data with information from other modalities to generate polychromatic views of biological systems. For example, the amalgamation of molecular localization data, from fluorescence microscopy or spectromicroscopy, with structural information from X-ray tomography. This combination of data from the same specimen generates a more complete picture of the system than can be obtained by a single microscopy method. Such multimodal combinations greatly enhance our understanding of biology by combining physiological and morphological data to create models that more accurately reflect the complexities of life.

Keywords

X-ray; cryogenic; correlated; fluorescence; imaging; tomography

Introduction

Measurement of cell morphology, generally known as morphometry, is central to cell biology, medical research and clinical medicine. For example, morphometry is the basis for cell cycle analysis [1, 2], a guiding factor in cell culture experiments [3] and the standard method for differentiating between benign and malignant tumor cells [4]. Cell morphology also plays a key role in staging cancer and predicting how aggressively a tumor will grow and spread [5] since cell shape regulates gene function during carcinogenesis [6].

Imaging has proven to be an efficient, accurate method of quantifying both the internal (organelles) and external (cell shape) morphology of biological specimens [7, 8]. Over time, many different imaging modalities have been applied to morphometric studies, each with inherent strengths and weaknesses and capable of producing a sub-set of information about the specimen. Most commonly, light- and electron-based microscopy have been used to

analyze a cell's external size and shape, together with internal characteristics such as the number, shape and relative position of organelles and labeled molecules. However, even powerful modalities such as these have limitations, both regarding the type of specimens they can image and the information they can generate. As a result, much effort has gone into developing new modalities for making morphometric measurements on cells and filling gaps in information that can't be accessed by existing methods, even when they are applied in tandem to the same specimen [9–11].

An obvious path towards meeting this goal lies in the choice of specimen illumination. Bright-field light microscopes are limited in spatial resolution by the wavelength of light [12]. Fluorescence microscopes can image beyond the 'diffraction limit' imposed by the wavelength of the illumination, but they can only image labeled cellular structures or molecules, leaving the other cell contents dark [13–15]. Electron microscopes can only image thin specimens; cells larger than small bacteria must be sliced into sections that are less than 500 microns thick [16]. X-ray illumination has the potential to overcome these limitations and image all cell components in fully intact cells and do so with high spatial resolution [17]. Of course, X-rays have a storied history in clinical medicine and materials science [18]. However, for many years X-ray microscopes failed to live up to their early promise for imaging cell-scaled biological specimens at high spatial resolution[18]. Realizing this goal required developments in nanofabrication, detectors, cryopreservation and instrument design. Fortunately, these technological advances have now been made, and soft X-ray microscopy is now gaining influence and recognition as a tool for making morphological measurements on single cells, including large eukaryotic cells.

We should point out; this review is not meant to be a general overview of X-ray microscopy, for example, we do not discuss work carried out on biology at larger than the cellular scale or discuss the use of these instruments in research fields such as materials science and magnetism. The application of X-ray microscopy in these areas is profound and has produced enormous literature. Instead, we limit our discussion to the benefits of using X-rays to visualize and quantify the internal and external morphology of cells, in 3D and even 4D. We also describe the current combination of X-ray microscopy with other techniques, in particular, X-ray spectromicroscopy and light microscopy to add physiological information to morphological studies. Finally, we will look to the future, and the challenges of implementing higher-throughput, easier handling, and automated data analysis into biological X-ray microscopy.

Morphometrics: Historical perspective

Light microscopy

Humans can typically see objects in the size range of 6 to 20 μm, depending on age and eyesight [19]. So, at best we can see a large isolated eukaryotic cell but can't distinguish sub-cellular detail. That requires a magnifying device. The earliest example of this concept was Robert Hooke's observation in 1665 that cork is comprised of compartments or "cells" [20]. In the 200 years that followed, light microscopy gave us first sight of organisms, such as protozoa and bacteria, and key sub-cellular structures, such as the nucleus and mitochondria [21, 22]. Staining procedures - developed for light microscopy by Retzius in

1881 - laid the foundation for discovering the microscopic *anatomy* of cells and the establishment of histology [23. Light microscopy also provided the first morphological analyses of cells when bacterial pathogens that caused human diseases were described by microscopic observation of their shape by Koch, Klebs, and Pasteur {Blevins, 2010 #2788. Light microscopy also provided the first morphological analyses of cells when bacterial pathogens that caused human diseases were described by microscopic observation of their shape by Koch, Klebs, and Pasteur {Blevins, 2010 #2788]. Light microscopy was also the basis of many other landmark studies. Examples include the first quantitative study of the chromatin morphology during the cell cycle [24], the effect of insulin-like and epidermal growth factors on cell morphology [25], and the effect of varying osmolarities on the morphology of sickle cell [26]. These are but a few examples that highlight light microscopy for studying cell morphology. Nowadays, practically every light microscope can be equipped with analysis software for cell counting and cell morphology analysis, making these routine tasks in cell culture and histopathology. Light microscopy has the advantage of being able to image living specimens and generally requires minimal sample preparation. With the use of confocal and super-resolution light microscopy, one can partly overcome some inherent limitations of the technique, such as low spatial resolution, but obtaining a complete, unaltered 3D imaging of the internal cell morphology using light microscopy remains a challenge.

Electron microscopy

The discovery of electrons in 1897 by Thompson opened up the possibility of a microscope with three orders of magnitude better spatial resolution than light microscopes can achieve [27]. But the physical properties of electrons meant new, complex sample preparation protocols had to be developed for biological specimens. In an electron microscope, biological specimens have to withstand both the high vacuum needed to prevent deflection of electrons by air and elevated temperatures caused by the absorption of high energy electrons by the specimen [28, 29]Furthermore, the strong interaction of electrons with the specimen results in scattering of the illumination. This scattering limits the maximum thickness of biological specimen that can be imaged to less than a micron. The first two conditions can be mitigated by ‘fixing’ the specimen, the latter by sectioning. Protocols for epoxy embedding [30], sectioning of tissue [31] and chemical fixation protocols [32] enabled the early application of electron microscopy to cell imaging [33], and allowed, for example, the first observation of mitochondria, the Golgi apparatus, a structure later called ‘endoplasmic reticulum,’ together with the visualization of viruses and other sub-cellular structures [34–36]. With the establishment of methods for 3D tomographic data acquisition, together with protocols for cryogenic fixation, electron microscopy became - and remains - the gold standard for high-resolution biological imaging [35, 37–39]. The importance of electron microscopy in biology was recently recognized by the Nobel committee, with the 2017 Chemistry prize award to Joachim Frank, Richard Henderson, and Jacques Dubochet for the development of cryogenic electron microscopy (cryo-EM).

What was missing?

As highlighted above, light- and electron-based microscopes are fantastic tools that have made enormous contributions to our knowledge of cells and biological systems.

Nevertheless, their respective limitations result in information gaps, either because the necessary imaging data can't be obtained, or can only be obtained from a very small number of cells (as is the case in EM tomographic reconstructions of entire eukaryotic cells). From the perspective of cell imaging, there remained the need for methods that overcome the limitations of light and electron microscope. Specifically, an imaging technique with high spatial resolution and high penetration power for hydrated specimens, ideally with minimal sample preparation prior to imaging. In short, a technique that can measure the internal and external morphologies of large numbers of intact eukaryotic cells held in a near-native state. This and other unique

X-ray microscopy

Wilhelm Röntgen discovered X-rays in 1895, an achievement that earned him the Nobel prize in physics in 1901. The penetration power of X-rays was demonstrated in the famous image of the bones in the hand of Röntgen's wife, Anna Bertha Ludwig. The medical community responded to this image with enormous enthusiasm, and almost immediately adopted X-ray radiography as a clinical technique [40]. X-ray use is now ubiquitous in medicine, to the point most people in the developed world will have a clinical X-ray procedure at least once in their life.

Despite the promise of X-rays as the basis of new imaging methods for cell biology, the initial work was disappointing. X-rays have a very low refractive index in virtually all materials [41]. Therefore, it is impossible to use a conventional magnifying lens, such as those used in a light microscope to focus X-rays. As a result, X-ray imaging of biological specimens was limited in magnification, and not particularly informative [18, 42].

The modern era of biological X-ray microscopy began in the 1970s with the development of X-ray lithography and high-resolution detectors. Schmahl and co-workers built the first X-ray transmission microscope at the Deutsches Elektronen-Synchrotron (DESY), Hamburg [43–45]. Unlike its predecessors, this X-ray microscope produced high resolution and excellent contrast images of cells, even when they were imaging through a relatively thick water layer [46–49]. As a result of this success, several groups around the world were inspired to design, build and apply X-ray microscopes to take morphometric measurements from cell. Many excellent reviews are available that summarize developments and applications of X-ray microscopes [18, 42, 50–52].

These days, a diverse family of X-ray microscopes are available. There are now microscopes with illumination in the soft (under 1 keV) and hard (1 to 100 keV) X-ray energy regimes [41, 53]. These microscopes operate with either transmission or scanning geometries [41] with images being generated by a variety of different mechanisms, for example absorption, phase contrast, or even coherent diffraction. X-ray microscopes now offer imaging capabilities that are applicable in almost any research field. However, biological specimens present unique challenges compared to other types of specimen. Specifically, living organisms have a relatively low tolerance towards ionizing radiation as compared to materials science specimens, such as magnetic materials ***. Susceptibility to radiation damage held up the development of soft X-ray microscopy for biology for many years. But that hurdle was overcome by the development of cryogenic specimen stages that capable of

holding flash frozen cells at liquid nitrogen temperature during data acquisition ****. While this technology does not eliminate radiation damage completely, it mitigates it well enough to allow data collection to be completed long before damage becomes apparent in X-ray images. Before discussing this application in more detail, we should survey the landscape of available X-ray methods and their features.

From the cell biology perspective, X-ray microscopes fall into one of two categories, **full-field transmission** (visualize morphology) and **scanning** in 2D or 3D (to access physiology information) (see Table 1). In both categories of microscope soft and hard x-rays can be used, depending on the desired penetration depth, spatial resolution and contrast mechanism [54]. While there are multiple examples of using soft x-ray coherent diffraction imaging [55–61] and hard x-ray microscopy for visualizing cells [62–64] these techniques are mostly proof-of-principal studies and are not yet allowing the type of systematic studies required in cell biology. The preferred method for morphological studies of single cells is transmission soft x-ray microscopy.

Soft x-ray microscopy of cells

As we mentioned above, X-rays play a major role in many disciplines, including biology. Regarding the latter, X-ray microcomputed tomography and X-ray diffraction for protein crystallography are the most common uses of X-rays in biological research [65, 66]. In this review, however, we will hold focus on the class of transmission x-ray microscopes (TXM), which have a similar in optical design to light microscopes and use lenses to focus illuminating light onto the specimen and then use an objective lens to transmit a magnified image of the specimen onto a detector [41]. Since visible light and X-rays are electromagnetic radiation, the basic principles of bright-field light microscopy apply to X-rays in a TXM. Thus, obtaining high-quality imaging requires: bright, monochromatic illumination focussed to a spot approximately the same size as the specimen. In a TXM these criteria are met by using high-quality condenser and objective lenses, ideally with closely matched numerical apertures [67]. Also, the TXM must be fitted with a high sensitivity, low noise camera for detection and a specimen mounting system. In general, it is relatively easy to meet these criteria in light microscopy – indeed a vast amount of valuable science has been carried out using light microscopes with simple lenses and a human eye acting as the detector. However, in the context of X-rays, the situation is more complex. Developing TXMs as a biological imaging tool required the development of specialized X-ray lenses, the availability of brilliant X-ray sources, such as synchrotron radiation facilities [68] and many other technological advances as we will discuss below.

Nowadays, most TXMs are located at the synchrotron radiation facilities worldwide [69–71]. Here, we will skip discussing image formation and the basic principles of X-ray microscopy, all of which can be found in significant detail elsewhere [18, 41, 51, 72]. Instead, we will concentrate our attention on the criteria required for successful imaging of cell morphology with a TXM.

There is a common misconception that spatial resolution is the most important metric when assessing an imaging modality. This assumption is not limited to the TXM; it is a commonly

held belief about imaging modalities *per se*. And there is some logic to this assumption that *the more detail you can see, the better*. However, a more complete metric is to consider the information content of an image. As long as a microscope produces images that answer the questions being asked, the spatial resolution is somewhat irrelevant.

In transmission X-ray microscopy, illuminating photons are absorbed as they pass through the specimen. The spectral region that lies between the absorption edges of carbon (284 eV) and oxygen (540 eV) is termed the 'water window' [73]. In the water window, the absorption of X-ray photons by biological specimens adheres to Beer's Law and is therefore linear with concentration and molecular composition [71, 74]. Subsequently, highly solvated regions in a cell are relatively transmissive towards soft X-ray illumination. Conversely, regions such as membranes or condensed genetic material in the nucleus, which are dense with carbon-containing molecules absorb illuminating photons much more strongly. The resulting differential absorption of the illumination produces images contain quantitative information on every part of the specimen [75].

Soft X-rays have sufficient penetration depth for analysis of intact, fully hydrated cells. The relatively fast acquisition time enables relatively high-throughput imaging, essential for studies like the phenotyping of cells [71, 76–79]. 3D imaging of very large cells, tissues, and organisms require the greater penetration depth of hard X-rays. Up to now, X-ray projection tomography has demonstrated the most promising results for subcellular morphological imaging of 'thick specimens' [65, 80–82].

The strong interaction with organic material limits the penetration of soft X-rays to approximately 10–15μm, depending on the cell type [83]. Imaging cells or tissues thicker than this requires deformation of specimens, making them extended in one direction (for example flat or cylindrical objects that are thinner in some orientations) or trimming them to the suitable thickness as done in electron microscopy. Microscopy with hard x-rays overcomes the limitation on specimen thickness but relies on chemical staining or the use of phase contrast data acquisition protocols [84–86].

As in light microscopy, the depth of field of an X-ray microscope depends on the wavelength and numerical aperture of the objective. Higher resolution requires larger numerical aperture and consequently smaller depth of field. Thus, 3D imaging of a whole cell comes at the cost of spatial resolution achievable for the desired specimen thickness. Conventionally specimen trimming for soft X-ray microscopy or imaging with hard X-rays were used to overcome this limitation. However, several approaches have been proposed [87–91] to extend the depth of field in soft X-ray microscopy enabling in future to image larger cells with high resolution in 3D. These approaches are either based on the acquisition of additional through-focus projections, that is to say, similar to methods used in confocal microscopy, or rely on the computational methods to compensate for the limited depth of field.

Imaging contrast and depth of field (coupled with spatial resolution) can be pushed only to the extent of X-ray radiation dose which can be tolerated by the specimen. In most cases, the dosage required is lower than with electron microscopy [47]. However, the specimen is still estimated to be exposed to a dose as high as 10^7 Gy [92]. The effect of X-rays on biological

specimens is severe [93], but the damage can be mitigated by imaging at cryogenic temperatures [29, 46, 92, 94, 95]. Cryogenic temperatures used in biological X-ray microscopy to mitigate radiation damage requires only one step – vitrification. However, although straightforward, this step is a crucial determinant of image quality. Here, we would like to point out a few factors for successful sample preparation. The foremost requirement is to locate the cell or region of interest to freeze down. While this can be done later with the light microscopes integrated into X-ray microscopes, the most efficient way is to select cells of interest before vitrification, for example by techniques such as fluorescence-activated cell sorting [96]. Two (specimen) holder types are currently in use for TXM imaging of cells: thin-walled glass capillaries and grids developed for electron microscopy [97]. While the use of grids has the advantage of access to well-established, existing protocols from electron microscopy, grid mounted specimens are limited in possible rotation range by as much as ±30%, resulting in missing information in 3D data series and the generation of artifacts and reduction of the axial spatial resolution. On the other hand, capillary mounted specimens can be rotated without limitation to generate tilt series with no systematically missing data [98]. Independent of the holder type, the mounted specimen is frozen using methods developed for EM cryo preservation, such as freezing with a blast of cooled helium gas, plunge freezing or high-pressure freezing.

All aforementioned criteria are typically in the hands of experts in X-ray microscopy who developed the technique. However, there is an additional criterion, which depends on the “users,” most probably cell biologists, being able to recognize the specimen when they see it. Since contrast and resolution differ significantly from well-known imaging methods used in most laboratories (i.e., light and electron microscopy), one should be open-minded when interpreting X-ray microscopy data. TXM data contains new, never seen before information.

In the following sections, we will survey studies that analyzed both the internal and external morphology of cells. Many of these studies are based on quantitative morphological analysis, creating a niche for X-ray microscopy in the characterization of cellular architecture in 3D.

External Morphology

Cells are typically classified by their size, shape, and function. Size and shape are morphometric measurements, with the function being a physiological characterization.

Morphology is routinely used to differentiate and identify simple cells, such as bacteria. For example, the curved cell shape of *Caulobacter crescentus* easily distinguishes it from rod-shaped bacteria such as *Escherichia coli* [99]. In eukaryotic cells, the geometric characteristics are more complex, but the same basic principle holds. For example, fibroblasts are elongated; neurons are dendritic [100], and so on. Determining the 3D shape of cells is one of the most fundamental tasks in cell biology. Consequently, some automated high-throughput techniques have been designed for pathology [100, 101] and are indispensable for everyday clinical diagnostics. For fundamental cell biology, however, a highly detailed 3D picture of cell shape is often necessary, in addition to an averaged,

ensemble representation output by high-throughput methods. This is an area where SXT excels.

An example of external cell morphometrics

Red blood cells are known for their biconcave disc shape, and their deformation of normal shape serves as an indicator of sickle cell disease. About one in 4000 individuals are diagnosed with sickle cell disease only in the USA [102], preventive approaches or effective treatment strategies do not exist. Darrow et al. used soft X-ray microscopy to analyze the size and shape of over 600 sickled red blood cells throughout the progression of disease [103]. The number of protrusions, not accessible with 2D methods, was used as an indicator of the sickling severity and could be classified into four categories as a function of disease progression: none, mild, moderate and severe (Figure 1A). Furthermore, the group analyzed the effect of the anti-sickling drug compound 5C and showed that it could decrease the severity of the sickling disease in about 80% of cases. This work is a shining example of soft X-ray tomography being used to both classify disease states and the efficacy of candidate pharmaceuticals.

Internal Morphology

The real power of soft X-ray microscopy lies in the deep penetration depth of these photons and the contrast generated by using ‘water window’ illumination. In tandem, these two characteristics allow visualization and quantification of both the internal and external morphologies of intact cells. Where electron microscopy would require sectioning of the cells and light microscopy would need the use of multiple fluorescent tags, soft X-ray microscopy provides natural contrast based on X-ray linear attenuation coefficient of all organelles within a cell. The number and organization of organelles in a cell depends on its complexity and tissue type [104]. These characteristics also change quickly during the cell cycle, during development and in response to environmental factors such as cell density, temperature, oxygen concentration, and the availability of nutrients [105, 106].

Examples of studies quantifying the internal morphology of cells

Yeast is one of the simplest eukaryotic organisms, even so it undergoes many of the same essential processes as mammalian cells. Therefore, yeast has become a widely used model organism to study cell growth and division [107]. Yeast has been studied extensively using soft X-ray microscopy [62, 76, 77, 108–110]. Based on other methods, it was already established that ploidy (the number of complete sets of chromosomes) in yeast has a direct and linear proportionality on cell size. While cell size in both budding and fission yeast has been shown to be proportional to the growth of the nucleus, other organelles and their relation to ploidy of the fungal cells has been unknown. Uchida et al. have used soft X-ray microscopy to measure volumes of the cell and the significant organelles in both haploid and diploid strains of *S. cerevisiae* at the four stages of the yeast cell cycle [77]. Lipid bodies, mitochondria, vacuoles, nucleus, and nucleolus were visualized and measured in 3D at G1, S, G2 and M stages of the yeast cell cycle (Figure 1C). Except for vacuoles, the growth of the main classes of organelle was found to be strictly regulated with cell size at all stages of the cell cycle and in both haploid and diploid strains. These studies have shown that yeast possesses well-defined optimal volumetric ratios that are most probably independent of

strain, ploidy, and phenotype and these ratios are therefore common to all yeast cells. To analyze the underlying mechanism and functional importance of these constant ratios, Walters et al. used soft X-ray tomography to study nuclear to cell volumes in wild-type and arrested *cdc5-of* mutant budding yeast [111]. Both yeast cell types were staged in G1 and then released into media containing nocodazole (Figure 1B). As cells progressed towards a mitotic arrest, nuclear volume and surface area compared to cell size were measured (Figure 1D). Despite different morphologies of mutant and wild-type cells, nuclear surface area to cell volume increased at the same rate, suggesting that flare formation allows the cells to keep this ratio without altering its nuclear volume. Future soft X-ray microscopy studies on yeast mutant cells will deepen our understanding of how cells control their size and arrangement of organelles during the cell cycle.

X-ray microscopy has been also used to analyze structurally more complex cells, like green alga *Chlamydomonas reinhardtii* [17, 112], bacteria [113], lymphocyte T-cells [114] and olfactory neurons [115–117]. A Recent study demonstrated that quantitative analysis based on linear attenuation coefficient of X-rays is sensitive to biomolecular concentration, resolving substructure of organelles, particularly the nuclear organization inside stem cells [118]. Nuclear organization and chromatin conformation have been studied in embryonic and hematopoietic stem cells with varying lineage potential, particularly in embryonic stem cells, hematopoietic stem cells, multipotent progenitors, granulocyte/macrophage progenitors, B cells, and granulocyte/monocyte cells. While heterochromatin volume remained similar in all cell types, the euchromatin volume decreased significantly upon differentiation, suggesting that the nuclear size is determined predominantly by euchromatin. 3D analysis of nuclear shape and interface between chromatin and euchromatin revealed high nuclear folding and extensive chromatin interphase in the stem and progenitor cells indicating greater lineage potential. This chromatin compaction effect was further investigated during neurogenesis *in vivo* [117]. Advanced analysis of heterochromatin in nucleus showed unappreciated interconnectivity of hetero- and euchromatin in multipotent stem cell, neuronal progenitor, mature neuron and HP1β knock-out mature neuron of the olfactory epithelium cells (Figure 2A). It was shown that heterochromatin and euchromatin are highly interconnected (more than 98%) in all type of cells. This continues lattice-like structure of heterochromatin serves as an architectural platform to organize parts of euchromatin. Depletion of HP1β did not disrupt this continuity, despite reduced heterochromatin and its lost connections to the nuclear envelope. Thus, HP1β might regulate chromatin compaction, reorganization, and interactions with the nuclear envelope.

Such access to the ultrastructural organization in whole cells placed X-ray microscopy as a valuable tool to study cell-parasite interactions. Structural development of malaria parasite, for example, was extensively studied by several groups by 2D soft X-ray microscopy [119–121], soft X-ray coherent diffraction imaging }[122] and X-ray fluorescence diffraction [123, 124]. Spatial localization of vaccinia and herpes viral factories was likewise observed by X-ray microscopy [125–127]. Lately, ultrastructural alterations were studied in hepatitis C virus-infected cells [78]. While the nuclear envelope and liposomes in hepatitis C viral cells were unaltered in comparison to the typical cell, most striking differences were observed in the endoplasmic reticulum as enlarged cisternae, tubular structures, vesicular extrusions and multiple membrane vesicles (Figure 2B). The effect of clinically relevant

antiviral drugs such as telaprevir, daclatasvir, and sofosbuvir has partially reversed alterations of endoplasmic reticulum and mitochondria, suggesting that optimal antiviral drug combination could be useful in the treatment of chronic hepatitis C viral infection.

Collectively these results demonstrate the various ways by which soft X-ray microscopy is impacting our understanding of cell biology. The high spatial resolution, penetration of an entire even eukaryotic cell, imaging in the native state and 3D quantitative analysis of cell organelles are key features of this technique. analysis of multi-cellular structures.

Multi-cellular morphology

Biological processes rely not only on the morphology of each cell but also on the intricate balance of cell-cell or cell-environment interactions. Topics of ongoing research range from morpho- and organo-genesis to wound healing, cancer cell metastasis, and immune system reaction, to control cell-cell communication. Current studies demonstrate that the understanding of cell morphology is incomplete without understanding its microenvironment [128]. This is particularly true in the case of the nanoscale materials that are increasingly used in consumer goods can modulate cell morphology at the subcellular level [129]. Nanoparticles are of particular interest as biosensors and for the targeted delivery of cancer therapeutics [129]. Here, the natural contrast of soft X-ray microscopy offers a unique tool to visualize morphological cell in response to microenvironmental changes. Nanoparticle-cell interactions have been investigated in *Chlamydomonas* cells by near-edge soft X-ray microscopy [130] and in human skin by scanning transmission microscopy [131, 132].

Beyond qualitative visualization, Chiappi et al. demonstrated the use of soft X-ray tomography (SXT) for quantitative analysis of cell vesicles used for iron oxide nanoparticle uptake by breast cancer cells [133]. Size and distance between vesicles containing nanoparticles were evaluated at various incubation times (Figure 3A). The cells take up iron oxide nanoparticles rapidly towards the nucleus and then continuously increase the number and size of vesicles containing nanoparticles. Such a comprehensive quantitative analysis of the cell-nanoparticle interaction is beneficial for nanoparticle design and the specific development of those best suited for clinical applications.

While soft X-ray microscopy is superior in terms of natural contrast for visualization of cell organelles, it is limited to studying the morphology of a single cell or cell monolayers only. To visualize cell morphology in cell cultures, tissues, and organisms, X-ray microscopy is pushed towards using higher energy (i.e., harder) X-rays. At higher X-ray energies, absorption contrast is lost, and cells become transparent. For imaging of cellular morphology, hard X-ray microscopy thus relies on staining or phase contrast methods. As with electron microscopy, chemical staining for X-ray microscopy could be used to visualize the structure of cells [63]. But for imaging of morphological changes in cell-cell or cell-environment studies, chemical staining is a potential source of artifacts, making interpretation of the data unreliable. Phase-contrast microscopes overcome the problem of low absorption contrast and can image unstained cells in the native state. Hard X-ray microscopy has been already used to visualize chromatid concentration in the human chromosome [58] and the spatial organization of organelles in yeast spore cell [134].

Although the potential of hard X-ray microscopy has been demonstrated, examining cell-cell interactions within macroscopic tissue samples requires an X-ray microscope that can be "zoomed" to the cell of interest. Such phase-contrast zoom microscopy has been developed by the groups of Tim Saldit, Peter Cloetens and Lukas Helfen [135, 136]. Recently, they successfully localized and imaged macrophages in mouse lung tissues, analyzing barium-instilled macrophages distribution in healthy and asthmatic lung tissues [136]. The 3D reconstructions showed that macrophages localize predominantly in the alveolar lumen and are even able to migrate through the epithelial layer. Use of hard X-ray microscopy for morphological cell analysis of tissues overcomes time-consuming sectioning and histology, enabling visualization of morphological changes in a single cell within macroscopically thick multicellular tissues. Imaging cell-cell interactions *in vivo* using hard X-rays produces even greater insights into multicellular tissues and organisms. However, the required highly-damaging dose of X-rays has always been a barrier for such studies. Nevertheless, four-dimensional X-ray microscopy studies have been carried out successfully in small organisms, i.e., fly pupae [137], weevil joints [138] and frog embryos [139, 140]. While insects are more resistant to X-ray radiation [141], the 4D microscopy of the frog embryo required elaborated imaging experiments [140]. In the frog embryo study, morphology and movement of cells were captured by hard X-ray phase contrast microscopy during the gastrulation of *Xenopus laevis*. Cell shape and subcellular structures, such as nuclei and yolk platelets, were used to differentiate between ectoderm, mesoderm, and endoderm cell layers (Figure 3B). Furthermore, morphologically distinct cells were tracked during the gastrulation process, allowing discrimination between collective and relative cell motion. Such a global view on morphogenetic analysis helps relate to changes in cellular shape and forces regulating cell development towards a multi-layered organism.

The studies described above demonstrate the immense potential of soft and hard X-ray microscopy for the morphological analysis of multi-cellular systems. Though *in vivo* 3D imaging with submicrometer resolution is still not achieved, manifold applications can be envisioned for time-lapse analysis of the cell morphology, such as the response of cells to infection, the reaction of immune cells to cancer, migration of cancer cells in healthy tissue, and the response of cells exposed to materials such as nanoparticles or biomimetic scaffolds.

Connecting morphology with physiology

The X-ray techniques discussed so far are best suited to morphometric measurements. Still, this is only part of the story. Biologists also need physiological data, ideally measured from the same cell. This can be achieved by imaging trace elements using X-rays. Since element specificity depends on the energy of t[142]he incoming X-rays, the decision between using soft or hard X-rays is based on the element of interest. Despite challenges, like absorption of the emitted photons and the complexity of reconstructing 3D spectroscopic data, there is a growing number of applications for investigating the physiology of cells [143–145]. We would like to point out that this summary of methods is limited by space, and in no way approaching comprehensive coverage. For example, we do not discuss combinations or multimodal approaches, for example, X-ray ptychography and fluorescence imaging [144]. The exact resolution, penetration depth and time for 3D imaging will vary between X-ray microscopes, depending on the instrument, acquisitions geometries, available signal, and

type of specimen. Thus, we advise you to use the examples below as a guideline to find X-ray microscope beneficial to the question of interest and recommend contacting an expert in the corresponding field to guarantee success in applying X-ray microscopy your research.

Correlated light microscopy: Molecular localization

Cell morphometric data is of limited use without knowledge of cell function. Physiological processes, like motility, ion transport, metabolism, including protein location and associations are typically visualized by fluorescence light microscopy [146]. The recent development and commercialization of super-resolution fluorescence microscopy have enabled fluorescence imaging at the nanometer scale. Fluorescence microscopy is common to virtually every cell biology laboratory. Consequently, its correlation with X-ray microscopy is a natural progression. In fact, some of the early TXM publications relied on data acquired by both X-ray and fluorescence light microscopy for interpretation of the X-ray tomographic data [108]. Typically, fluorescence microscopy confirmed what had been discovered through X-ray microscopy, or vice versa. Accurate correlative imaging became possible thanks to the development of high numerical aperture cryogenic light microscopy [13]. The cryogenic specimen environment in this microscope significantly enhances the working lifetime of fluorescent proteins and molecules, allowing the collection of through-focus or even fluorescence tomography data. Using the cryo-light microscope allows analysis of the same vitrified specimen by fluorescence and X-ray microscopy. Correlated fluorescence and X-ray microscopy is an area of active development [75, 96, 147–152]. Early works linked the 3D structure of a cell with molecular localization data, for exmaple by identifying fluorescently-tagged inactive X chromosome in female thymic lymphoma cells in the context of a soft X-ray tomographic reconstruction [96], or following the dynamics of granule and vesicles in activated mast cells [153], and analyzing ER-mitochondria contacts [154].

The latter study followed morphological changes during mitochondria fission. Mitochondria are known to be highly dynamic organelles which undergo fission and fragmentation throughout the cell lifetime. Though some proteins have known to play a role in the fragmentation of mitochondria, their interplay and their connection with other organelles were studied recently by Elgass et al [154]. They used soft X-ray tomography to analyze the 3D structure of mitochondria and ER and linked it to the mitochondrial outer membrane proteins MiD49/51 by correlated cryogenic fluorescence microscopy (Figure 4A–C). 3D visualization showed that ER protrudes towards mitochondria using short fingerlike extensions, creating ER-mitochondria contact sites (Figure 4D–H). Fluorescence microscopy revealed that these contact sites contain membrane protein MiD51 GFP foci. Furthermore, quantitative analysis of the MiD51 expression level and X-ray linear attenuation coefficient allowed to differentiate fragmented and normal cell phenotype. Loss of constriction sites and lower protein concentrations were observed for the fragmented phenotype. These results suggest that either MiD expression or mitochondria fragmentation is involved in ER-mitochondria exchange [154].

Such 3D correlation of morphology with fluorescence expression links function of the cell with its ultrastructure. Upcoming combination of X-ray microscopy with super-resolution

microscopy will bring these methods to similar and isotropic spatial resolution, making this emerging modality superior for cell analysis.

Correlated X-ray fluorescence: major and trace elements

So far, we have discussed X-ray microscopy as a tool for imaging the distribution of three out of the “big four” molecular building blocks in a cell, i.e., carbon, oxygen, hydrogen, and nitrogen (X-rays are not sensitive to bond hydrogen). Using the water window with soft X-rays and the phase contrast technique available for hard X-rays both allow the analysis of the morphology of cells with sufficient contrast resulting from these elements. Addressing the overall physiology of cells requires the other factors essential for life and the function of the cells be imaged. Calcium, for example, is a messenger that helps to regulate multiple cellular functions such as secretion, contraction, cellular excitability and gene expression in all organs. Thus, calcium imaging in visible light microscopy was pioneered in 1980 by Tsien [155, 156]. Since then, calcium imaging has become the method of choice for imaging intracellular communications mainly in neural tissue [157, 158]. Zinc represents another primary element, which has a broad range of functions in various cellular processes, such as replication and repair, transcription and translation, metabolism and signaling, cell proliferation and apoptosis [159]. It has also been widely used in imaging, as an artificial transcription factor and even as specific modules for protein recognition [160]. Indeed, other significant elements like phosphorus, sulfur, and magnesium are also essential for studies on DNA and protein folding and signaling. Unlike these major elements, trace elements like iron, molybdenum, silicon, and others constitute just 0.5% of the cells in organisms. Still, this small fraction exerts a tremendous influence on all functions of cells [161].

Many highly sensitive microanalytical techniques and instruments have been developed for *in situ* analysis of major and trace elements [162]. Among them, X-ray fluorescence imaging offers the best combination of sensitivity and spatial resolution. Even though the radiation dose hinders *in vivo* X-ray fluorescence imaging, the ability to quantitively analyze all major and trace elements with one measurement lead to the development of X-ray spectromicroscopy as a stand-alone technique.

On the one hand, X-ray spectromicroscopy allows 3D imaging of the cell morphology. On the other hand, the energy scan performed while image acquisition gives access to different elements present in the physical volume of the cell. Thus, functional elements can be localized within the cell structure. Such correlative X-ray microscopy was traditionally used to address environmental impact by imaging uptake of trace elements in plant and marine cells [163, 164]. Sviben et al. showed that the unicellular organism *E. huxleyi* concentrate large amounts of calcium in a vacuole-like compartment [165]. Co-localized with calcium, high concentrations of phosphorus and minor levels of other cations may explain why *E. huxley* is thriving in waters with a low amount of phosphorus, where other phytoplankton cannot survive. Subcellular partitioning and allocation of Calcium ions within the 3D volume allowed the development of a conceptual model for the calcium pathway.

Similar to imaging unicellular organisms, X-ray spectromicroscopy can be applied to multicellular organisms and tissues to determine the intracellular distribution of metals such as iron, copper, and zinc.

Kim and co-workers correlated elements in *X.laevis* oocytes as they mature and initiate embryonic development [166]. The total number of atoms per cell at each developmental stage has shown that copper and zinc levels both rise significantly during meiotic stages, making zinc among three other transition metals the most abundant and crucial for healthy development.

More importantly, trace elements can be linked to the pathology of various diseases. The relationship between iron biochemistry and Alzheimer's disease in intact cortex from a mouse model has been recently investigated by Telling et al. [167]. Here, X-ray spectromicroscopy helped to identify that iron biomaterial deposits in the cortical tissue as magnetite. This demonstrates that iron reduced to a pure ferrous state is associated with the amyloid complex, which is a signature characteristic of Alzheimer's disease. This observation may lead to the development of novel iron-modifying therapy strategies for Alzheimer's disease. Altered levels of iron have also been proposed to be involved in other pathological condition, i.e., cataract formation [168]. Here, the distribution of 23 elements, metals, and other trace elements was visualized in the eye of a zebrafish wild-type and mutant embryos (Figure 4I). Many elements were highly enriched in the pigment epithelial layer in a wild-type embryo but were eliminated in knockdown of the zebrafish. These results suggest that by buffering trace elements, melanosomes in pigment epithelial cells protect the lens from stress during eye development.

The main advantages of X-ray spectromicroscopy are subcellular resolution and a high degree of chemical specificity in unstained or chemical stained specimens. With the ongoing research on acquisition strategies, 3D reconstruction algorithms and the development of X-ray spectromicroscopy for *in vivo* imaging [124, 169, 170], the correlation of major and trace elements at the subcellular level is a promising method for a fundamental understanding of the roles of the different components within the cell, cell toxicity studies in connection to worsened environmental factors, and the etiology of diseases.

Conclusion and Summary

X-ray imaging is continuing its rapid evolution as a tool for measuring cell morphology. Though constantly expanding, the technological concept of X-ray microscopy is established and well understood. By itself and in combination with fluorescence light microscopy, it has been applied to almost all cell types and tissues [72]. It is time to look broader and to challenge our current understanding of cell morphology. The exact number of organelles inside of the cell is surprisingly still unknown. With the discovery of membrane-less organelles, it seems to be a right time to draw a new 3D map of cell structure. In combination with visible light and electrons, X-ray microscopy paves a way to a comprehensive 3D phenotyping of cells. The human cell atlas within Chan-Zuckerberg initiative and multi-scale model of the human pancreatic beta cell are two examples of such pioneering works [171]. With such need for X-ray microscopy, its future is predestined to be a new "workhorse" for 3D phenotypic analysis of cells.

Looking to the Future

"Automation of the acquisition and interpretation of data in microscopy has been a focus of biomedical research for almost a decade." You might imagine this statement came from a recent publication or talk. However, it is the opening sentence of a paper by Prewitt and Mendelson published in 1966 [172]. The most valuable imaging techniques provide high content, fast, reproducible and reliable, ideally with moderate effort, data on the specimen of interest. X-ray microscopy is not an exception. State of the art X-ray microscopes offers a quantitative analysis of the external and internal morphology of cells, cell cultures, and even organism. They are indispensable to look at cells in 3D. However, three fundamental components, initially outlined by Prewitt and Mendelsohn, remain unresolved for X-ray microscopy. Primarily, most operating X-ray microscopes for biological research are located at synchrotron facilities, making them hard to access and not a complement to day-to-day imaging techniques used in most laboratories. Ideally, table-top scale X-ray microscopes should be collocated with light microscopes on and accessible at any time of the day. Current development of table-top and compact X-ray sources initiated first laboratory X-ray microscopy prototypes and proof-of-principal experiments [80, 173]. The only commercialization of such X-ray microscopes, ideally at the affordable scale, can assure it's benefit to cell biology. The next component is automated data processing, such as online tomographic reconstructions and automatic segmentation. To some extent, algorithms and pipelines can be adopted from the existing fast X-ray tomography routines [174, 175]. However, for routine and reliable use, they have to be optimized for X-ray microscopy data [176]. The last but not the least is an automatic analysis of discrimination criteria. While looking at the beautiful 3D visualization of cell morphology is genuinely fascinating at the first time, it is not as stunning at the 100^{th} of them, especially if it should be annotated, measured and compared to other datasets. Likely, all these developments will come soon with active users of X-ray microscopy.

Acknowledgments

V.W. is supported by German Research Foundation research fellowship WE 6221/1–1. The National Center for X-ray Tomography is supported by NIH (P41GM103445), DOE's Office of Biological and Environmental Research (DE-AC02–5CH11231) and the Gordon and Betty Moore Foundation.

References

1. Calvert ME, Lannigan JA, Pemberton LF (2008) Optimization of yeast cell cycle analysis and morphological characterization by multispectral imaging flow cytometry. Cytometry A. 73, 825–33. 10.1002/cyto.a.20609 [PubMed: 18613038]
2. Stacey DW, Hitomi M, Kanovsky M, Gan L, Johnson EM (1999) Cell cycle arrest and morphological alterations following microinjection of NIH 3T3 cells with pur alpha. Oncogene. 18, 4254–61. 10.1038/sj.onc.1202795 [PubMed: 10435638]
3. Cooper WG (1965) Handbook of cell and organ culture. Am Sci. 53, A123–&.
4. El-Naggar AK, Chan JKC, Takata T, Grandis JR, Slootweg PJ (2017) The fourth edition of the head and neck world health organization blue book: Editors' perspectives. Hum Pathol. 66, 10–2. 10.1016/j.humpath.2017.05.014 [PubMed: 28583885]
5. Muzzio NE, Carballido M, Pasquale MA, Gonzalez PH, Azzaroni O, Arvia AJ (2018) Morphology and dynamics of tumor cell colonies propagating in epidermal growth factor supplemented media. Phys Biol. 15, 046001 10.1088/1478-3975/aabc2f [PubMed: 29624182]

6. Sailem HZ, Bakal C (2017) Identification of clinically predictive metagenes that encode components of a network coupling cell shape to transcription by image-omics. Genome Res. 27, 196–207. 10.1101/gr.202028.115 [PubMed: 27864353]
7. Ryan J, Gerhold AR, Boudreau V, Smith L, Maddox PS (2017) Introduction to modern methods in light microscopy. Methods Mol Biol. 1563, 1–15. 10.1007/978-1-4939-6810-7_1 [PubMed: 28324598]
8. Kherlopian AR, Song T, Duan Q, Neimark MA, Po MJ, Gohagan JK, Laine AF (2008) A review of imaging techniques for systems biology. BMC Syst Biol. 2, 74 10.1186/1752-0509-2-74 [PubMed: 18700030]
9. Ellisman MH, Deerinck TJ, Shu X, Sosinsky GE (2012) Picking faces out of a crowd: Genetic labels for identification of proteins in correlated light and electron microscopy imaging. Methods Cell Biol. 111, 139–55. 10.1016/B978-0-12-416026-2.00008-X [PubMed: 22857927]
10. Kim D, Deerinck TJ, Sigal YM, Babcock HP, Ellisman MH, Zhuang X (2015) Correlative stochastic optical reconstruction microscopy and electron microscopy. PLoS One. 10, e0124581 10.1371/journal.pone.0124581 [PubMed: 25874453]
11. Martone ME, Deerinck TJ, Yamada N, Bushong E, Ellisman MH (2000) Correlated 3d light and electron microscopy: Use of high voltage electron microscopy and electron tomography for imaging large biological structures. J Histotechnol. 23, 261–70.
12. Abbe E (1873) Beiträge zur theorie des mikroskops und der mikroskopischen wahrnehmung. Arch Mikrosk Anat. 9, 413–68.
13. Le Gros MA, McDermott G, Uchida M, Knoechel CG, Larabell CA (2009) High-aperture cryogenic light microscopy. J Microsc. 235, 1–8. 10.1111/j.1365-2818.2009.03184.x [PubMed: 19566622]
14. McDermott G, Le Gros MA, Knoechel CG, Uchida M, Larabell CA (2009) Soft x-ray tomography and cryogenic light microscopy: The cool combination in cellular imaging. Trends Cell Biol. 19, 587–95. 10.1016/j.tcb.2009.08.005 [PubMed: 19818625]
15. McDermott G, Le Gros MA, Larabell CA (2012) Visualizing cell architecture and molecular location using soft x-ray tomography and correlated cryo-light microscopy. Annu Rev Phys Chem. 63, 225–39. 10.1146/annurev-physchem-032511-143818 [PubMed: 22242730]
16. Leis A, Rockel B, Andrees L, Baumeister W (2009) Visualizing cells at the nanoscale. Trends Biochem Sci. 34, 60–70. [PubMed: 19101147]
17. Weiß D, Schneider G, Niemann B, Guttmann P, Rudolph D, Schmahl G (2000) Computed tomography of cryogenic biological specimens based on x-ray microscopic images. Ultramicroscopy. 84, 185–97. [PubMed: 10945329]
18. Kirz J, Jacobsen C (2009) The history and future of x-ray microscopy. Journal of Physics: Conference Series. 186, 012001 10.1088/1742-6596/186/1/012001
19. Silverstein LD (2008) Foundations of vision. Color Research & Application. 21, 142–4. 10.1002/col.5080210213
20. Lane N (2015) The unseen world: Reflections on leeuwenhoek (1677) ‘concerning little animals’. Philos Trans R Soc Lond B Biol Sci. 370 10.1098/rstb.2014.0344
21. Ernster L, Schatz G (1981) Mitochondria: A historical review. J Cell Biol. 91, 227s–55s. [PubMed: 7033239]
22. Pederson T (2011) The nucleus introduced. Cold Spring Harb Perspect Biol. 3 10.1101/cshperspect.a000521
23. Gurcan MN, Boucheron LE, Can A, Madabhushi A, Rajpoot NM, Yener B (2009) Histopathological image analysis: A review. IEEE Rev Biomed Eng. 2, 147–71. 10.1109/RBME.2009.2034865 [PubMed: 20671804]
24. Sawicki W, Rowinski J, Swenson R (1974) Change of chromatin morphology during the cell cycle detected by means of automated image analysis. J Cell Physiol. 84, 423–8. 10.1002/jcp.1040840310 [PubMed: 4140195]
25. Miyata Y (1988) Growth factor- and phorbol ester-induced changes in cell morphology analyzed by digital image processing*1. Exp Cell Res. 175, 286–97. 10.1016/0014-4827(88)90193-0 [PubMed: 3282897]

26. Hijiva N, Horiuchi K, Asakura T (1990) Morphology of sickled cells produced in solution with varying osmolarity. J Pediatr Hematol Oncol. 12, 106 10.1097/00043426-199021000-00021
27. Gordon RE (2014) Electron microscopy: A brief history and review of current clinical application. Methods Mol Biol. 1180, 119–35. 10.1007/978-1-4939-1050-2_7 [PubMed: 25015145]
28. Glaeser RM (2016) How good can cryo-em become? Nat Methods. 13, 28–32. 10.1038/nmeth.3695 [PubMed: 26716559]
29. Glaeser RM, Taylor KA (1978) Radiation damage relative to transmission electron microscopy of biological specimens at low temperature: A review. J Microscopy. 112, 127–38.
30. Glauert AM, Glauert RH, Rogers GE (1956) A new embedding medium for electron microscopy. Nature. 178, 803 10.1038/178803a0
31. Hillier J, Gettner ME (1950) Sectioning of tissue for electron microscopy. Science. 112, 520–3. 10.1126/science.112.2914.520 [PubMed: 14787452]
32. Palade GE (1952) A study of fixation for electron microscopy. J Exp Med. 95, 285–98. 10.1084/jem.95.3.285 [PubMed: 14927794]
33. Allen TD (1979) Electron microscopy in human medicine. Br J Cancer. 40, 957-. 10.1038/bjc.1979.293
34. Porter KR, Claude A, Fullam EF (1945) A study of tissue culture cells by electron microscopy : Methods and preliminary observations. J Exp Med. 81, 233–46. 10.1084/jem.81.3.233 [PubMed: 19871454]
35. Goldsmith CS, Miller SE (2009) Modern uses of electron microscopy for detection of viruses. Clin Microbiol Rev. 22, 552–63. 10.1128/CMR.00027-09 [PubMed: 19822888]
36. Masters BR History of the electron microscope in cell biology Encyclopedia of life sciences: John Wiley & Sons, Ltd; 2009.
37. Oczypok EA, Oury TD (2015) Electron microscopy remains the gold standard for the diagnosis of epithelial malignant mesothelioma: A case study. Ultrastruct Pathol. 39, 153–8. 10.3109/01913123.2014.960542 [PubMed: 25268063]
38. Pusiol T, Franceschetti I, Scialpi M, Piscioli I, Tardio ML (2010) Electron microscopy: The gold standard in the differential diagnosis of chromophobe renal cell carcinoma and oncocytoma. Anal Quant Cytol Histol. 32, 58–60. [PubMed: 20701089]
39. Kim YJ, Kim HD, Park C, Park T, Kim J, Choi YJ, Kim YS, Lee KH, Kang CJ (2008) Morphological analysis of cells by scanning electron microscopy. Jpn J Appl Phys. 47, 1325–8. 10.1143/Jjap.47.1325
40. Scatliff JH, Morris PJ (2014) From roentgen to magnetic resonance imaging: The history of medical imaging. N C Med J. 75, 111–3. [PubMed: 24663131]
41. Attwood DT Soft x-rays and extreme ultraviolet radiation: Principles and applications. Cambridge, New York: Cambridge Uhiversity Press; 1999 470 p.
42. Kirz J, Jacobsen C, Howells M (1995) Soft x-ray microscopes and their biological applications. Q Rev Biophys. 28, 33–130. [PubMed: 7676009]
43. Niemann B, Rudolph D, Schmahl G (1976) X-ray microscopy with synchrotron radiation. Appl Opt. 15, 1883–4. [PubMed: 20165284]
44. Niemann B, Rudolph D, Schmahl G (1974) Soft-x-ray imaging zone plates with large zone numbers for microscopic and spectroscopic applications. Opt Commun. 12, 160–3. Doi 10.1016/0030-4018(74)90381-2
45. Niemann B, Rudolph D, Schmahl G (1976) X-ray microscopy with synchrotron radiation. Appl Opt. 15, 1883–4. 10.1364/AO.15.001883 [PubMed: 20165284]
46. Sayre D, Kirz J, Feder R, Kim DM, Spiller E (1977) Transmission microscopy of unmodified biological-materials - comparative radiation dosages with electrons and ultrasoft x-ray photons. Ultramicroscopy. 2, 337–49. [PubMed: 919076]
47. Sayre D, Kirz J, Feder R, Kim DM, Spiller E (1977) Potential operating refion for ultrasoft x-ray microscopy of biological materials Science. 196, 1339–40. [PubMed: 867033]
48. Sayre D, Kirz J, Feder R, Kim DM, Spiller E (1976) Transmission microscopy of unmodified biological materials. Comparative radiation dosages with electrons and ultrasoft x-ray photons. Ultramicroscopy. 2, 337–49. 10.1016/s0304-3991(76)91997-5

49. Sayre D, Kirz J, Feder R, Kim DM, Spiller E (1977) Potential operating region for ultrasoft x-ray microscopy of biological materials. Science. 196, 1339–40. 10.1126/science.867033 [PubMed: 867033]
50. Jacobsen C (1999) Soft x-ray microscopy. Trends Cell Biol. 9, 44–7. 10.1016/s0962-8924(98)01424-x [PubMed: 10087616]
51. Jacobsen C, Kirz J (1998) X-ray microscopy with synchrotron radiation. Nat Struct Biol. 5 Suppl, 650–3. 10.1038/1341 [PubMed: 9699617]
52. Sayre D, Chapman HN (1995) X-ray microscopy. Acta Crystallogr A. 51 (Pt 3), 237–52. 10.1107/s0108767394011803 [PubMed: 7779327]
53. Sakdinawat A, Attwood D (2010) Nanoscale x-ray imaging. Nat Photonics. 4, 840–8. 10.1038/nphoton.2010.267
54. Kaulich B, Thibault P, Gianoncelli A, Kiskinova M (2011) Transmission and emission x-ray microscopy: Operation modes, contrast mechanisms and applications. J Phys Condens Matter. 23, 083002 10.1088/0953-8984/23/8/083002 [PubMed: 21411893]
55. Miao J, Hodgson KO, Ishikawa T, Larabell CA, LeGros MA, Nishino Y (2003) Imaging whole escherichia coli bacteria by using single-particle x-ray diffraction. Proc Natl Acad Sci U S A. 100, 110–2. [PubMed: 12518059]
56. Miao J, Ishikawa T, Robinson IK, Murnane MM (2015) Beyond crystallography: Diffractive imaging using coherent x-ray light sources. Science. 348, 530–5. 10.1126/science.aaa1394 [PubMed: 25931551]
57. Miao JW, Sandberg RL, Song CY (2012) Coherent x-ray diffraction imaging. IEEE J Sel Top Quantum Electron. 18, 399–410. Doi 10.1109/Jstqe.2011.2157306
58. Nishino Y, Takahashi Y, Imamoto N (2009) Three-dimensional visualization of a human chromosome using coherent x-ray diffraction. Phys Rev Lett. 102 10.1103/PhysRevLett.102.018101
59. Huang X, Nelson J, Kirz J, Lima E, Marchesini S, Miao H, Neiman A, Shapiro D, Steinbrener J, Stewart A, Turner J, Jacobsen C (2009) Soft x-ray diffraction microscopy of a frozen hydrated yeast cell. Phys Rev Lett. 103 10.1103/PhysRevLett.103.198101
60. Marchesini S, Chapman H, Hau-Riege S, London R, Szoke A, He H, Howells M, Padmore H, Rosen R, Spence J, Weierstall U (2003) Coherent x-ray diffractive imaging: Applications and limitations. Opt Express. 11, 2344–53. 10.1364/oe.11.002344 [PubMed: 19471343]
61. Nelson J, Huang X, Steinbrener J, Shapiro D, Kirz J, Marchesini S, Neiman AM, Turner JJ, Jacobsen C (2010) High-resolution x-ray diffraction microscopy of specifically labeled yeast cells. Proc Natl Acad Sci U S A. 107, 7235–9. 10.1073/pnas.0910874107 [PubMed: 20368463]
62. Zheng T, Li W, Guan Y, Song X, Xiong Y, Liu G, Tian Y (2012) Quantitative 3d imaging of yeast by hard x-ray tomography. Microsc Res Tech. 75, 662–6. 10.1002/jemt.21108 [PubMed: 22505187]
63. Liang Z, Guan Y, Chen S, Tian Y (2015) Whole cells imaged by hard x-ray transmission microscopy. Fungal Biology. 89–107. 10.1007/978-3-319-22437-4_5
64. Yang Y, Li W, Liu G, Zhang X, Chen J, Wu W, Guan Y, Xiong Y, Tian Y, Wu Z (2010) 3d visualization of subcellular structures of schizosaccharomyces pombe by hard x-ray tomography. J Microsc. 240, 14–20. 10.1111/j.1365-2818.2010.03379.x [PubMed: 21050209]
65. Withers PJ (2007) X-ray nanotomography. Materials today. 10, 26–34.
66. Shi Y (2014) A glimpse of structural biology through x-ray crystallography. Cell. 159, 995–1014. 10.1016/j.cell.2014.10.051 [PubMed: 25416941]
67. Schmahl G (1983) X-ray microscopy. Proc Int Symp.
68. Bilderback DH, Elleaume P, Weckert E (2005) Review of third and next generation synchrotron light sources. Journal of Physics B-Atomic Molecular and Optical Physics. 38, S773–S97. 10.1088/0953-4075/38/9/022
69. Ekman AA, Chen JH, Guo J, McDermott G, Le Gros MA, Larabell CA (2017) Mesoscale imaging with cryo-light and x-rays: Larger than molecular machines, smaller than a cell. Biol Cell. 109, 24–38. 10.1111/boc.201600044 [PubMed: 27690365]

70. Do M, Isaacson SA, McDermott G, Le Gros MA, Larabell CA (2015) Imaging and characterizing cells using tomography. Arch Biochem Biophys. 581, 111–21. 10.1016/j.abb.2015.01.011 [PubMed: 25602704]
71. McDermott G, Fox DM, Epperly L, Wetzler M, Barron AE, Le Gros MA, Larabell CA (2012) Visualizing and quantifying cell phenotype using soft x-ray tomography. BioEssays. 34, 320–7. 10.1002/bies.201100125 [PubMed: 22290620]
72. Harkiolaki M, Darrow MC, Spink MC, Kosior E, Dent K, Duke E (2018) Cryo-soft x-ray tomography: Using soft x-rays to explore the ultrastructure of whole cells. Emerging Topics in Life Sciences. 2, 81–92. 10.1042/etls20170086
73. Le Gros MA, McDermott G, Larabell CA (2005) X-ray tomography of whole cells. Curr Opin Struct Biol. 15, 593–600. 10.1016/j.sbi.2005.08.008 [PubMed: 16153818]
74. Larabell CA, Nugent KA (2010) Imaging cellular architecture with x-rays. Curr Opin Struct Biol. 20, 623–31. 10.1016/j.sbi.2010.08.008 [PubMed: 20869868]
75. Le Gros MA, Knoechel CG, Uchida M, Parkinson DY, McDermott G, Larabell CA 2.6 visualizing sub-cellular organization using soft x-ray tomography In: Edward HE, editor. Comprehensive biophysics. Amsterdam: Elsevier; 2012 p. 90–110.
76. Uchida M, McDermott G, Wetzler M, LeGros MA, Myllys M, Knoechel C, Barron AE, Larabell CA (2010) Soft x-ray tomography of candida albicans treated with antifungal peptoids. Abstr Pap Am Chem Soc. 239.
77. Uchida M, Sun Y, McDermott G, Knoechel C, Le Gros MA, Parkinson D, Drubin DG, Larabell CA (2011) Quantitative analysis of yeast internal architecture using soft x-ray tomography. Yeast. 28, 227–36. 10.1002/yea.1834 [PubMed: 21360734]
78. Perez-Berna AJ, Rodriguez MJ, Chichon FJ, Friesland MF, Sorrentino A, Carrascosa JL, Pereiro E, Gastaminza P (2016) Structural changes in cells imaged by soft x-ray cryo-tomography during hepatitis c virus infection. ACS Nano. 10, 6597–611. 10.1021/acsnano.6b01374 [PubMed: 27328170]
79. Sorrentino A, Nicolas J, Valcarcel R, Chichon FJ, Rosanes M, Avila J, Tkachuk A, Irwin J, Ferrer S, Pereiro E (2015) Mistral: A transmission soft x-ray microscopy beamline for cryo nano-tomography of biological samples and magnetic domains imaging. J Synchrotron Radiat. 22, 1112–7. 10.1107/S1600577515008632 [PubMed: 26134819]
80. Muller M, de Sena Oliveira I, Allner S, Ferstl S, Bidola P, Mechlem K, Fehringer A, Hehn L, Dierolf M, Achterhold K, Gleich B, Hammel JU, Jahn H, Mayer G, Pfeiffer F (2017) Myoanatomy of the velvet worm leg revealed by laboratory-based nanofocus x-ray source tomography. Proc Natl Acad Sci U S A. 114, 12378–83. 10.1073/pnas.1710742114 [PubMed: 29109262]
81. Olendrowitz C, Bartels M, Krenkel M, Beerlink A, Mokso R, Sprung M, Salditt T (2012) Phase-contrast x-ray imaging and tomography of the nematode caenorhabditis elegans. Phys Med Biol. 57, 5309–23. 10.1088/0031-9155/57/16/5309 [PubMed: 22853964]
82. Bartels M, Krenkel M, Cloetens P, Mobius W, Salditt T (2015) Myelinated mouse nerves studied by x-ray phase contrast zoom tomography. J Struct Biol. 192, 561–8. 10.1016/j.jsb.2015.11.001 [PubMed: 26546551]
83. Le Gros MA, McDermott G, Larabell CA (2005) X-ray tomography of whole cells. Curr Opin Struct Biol. 15, 593–600. 10.1016/j.sbi.2005.08.008 [PubMed: 16153818]
84. Morrison GR, Niemann B (1998) Differential phase contrast x-ray microscopy. X-Ray Microscopy and Spectromicroscopy. 85–94. 10.1007/978-3-642-72106-9_10
85. Chen H, Wang Z, Gao K, Hou Q, Wang D, Wu Z (2015) Quantitative phase retrieval in x-ray zernike phase contrast microscopy. J Synchrotron Radiat. 22, 1056–61. 10.1107/S1600577515007699 [PubMed: 26134811]
86. Yang Y, Cheng Y, Heine R, Baumbach T (2016) Contrast transfer functions for zernike phase contrast in full-field transmission hard x-ray microscopy. Opt Express. 24, 6063–70. 10.1364/OE.24.006063 [PubMed: 27136800]
87. Liu Y, Wang J, Hong Y, Wang Z, Zhang K, Williams PA, Zhu P, Andrews JC, Pianetta P, Wu Z (2012) Extended depth of focus for transmission x-ray microscope. Opt Lett. 37, 3708–10. 10.1364/OL.37.003708 [PubMed: 22940998]

88. Li F, Guan Y, Xiong Y, Zhang X, Liu G, Tian Y (2017) Method for extending the depth of focus in x-ray microscopy. Opt Express. 25, 7657–67. 10.1364/OE.25.007657 [PubMed: 28380885]

89. Selin M, Fogelqvist E, Werner S, Hertz HM (2015) Tomographic reconstruction in soft x-ray microscopy using focus-stack back-projection. Opt Lett. 40, 2201–4. 10.1364/OL.40.002201 [PubMed: 26393699]

90. Oton J, Pereiro E, Conesa JJ, Chichon FJ, Luque D, Rodriguez JM, Perez-Berna AJ, Sorzano CO, Klukowska J, Herman GT, Vargas J, Marabini R, Carrascosa JL, Carazo JM (2017) Xtend: Extending the depth of field in cryo soft x-ray tomography. Sci Rep. 7, 45808 10.1038/srep45808 [PubMed: 28374769]

91. Ekman A, Weinhardt V, Chen JH, McDermott G, Le Gros MA, Larabell C (2018) Psf correction in soft x-ray tomography. J Struct Biol. 204, 9–18. 10.1016/j.jsb.2018.06.003 [PubMed: 29908247]

92. Shinohara K, Ito A (1991) Radiation damage in soft x-ray microscopy of live mammalian cells. J Microsc. 161, 463–72. 10.1111/j.1365-2818.1991.tb03104.x [PubMed: 2046092]

93. Kosior E, Cloetens P, Devès G, Ortega R, Bohic S (2012) Study of radiation effects on the cell structure and evaluation of the dose delivered by x-ray and α-particles microscopy. Appl Phys Lett. 101, 263102 10.1063/1.4773181

94. Schneider G (1998) Cryo x-ray microscopy with high spatial resolution in amplitude and phase contrast. Ultramicroscopy. 75, 85–104. [PubMed: 9836467]

95. Howells MR, Beetz T, Chapman HN (2009) An assessment of the resolution limitation due to radiation-damage in x-ray diffraction microscopy. J El Spec Rel Phen. 170 10.1016/j.elspec.2008.10.008

96. Smith EA, McDermott G, Do M, Leung K, Panning B, Le Gros MA, Larabell CA (2014) Quantitatively imaging chromosomes by correlated cryo-fluorescence and soft x-ray tomographies. Biophys J. 107, 1988–96. 10.1016/j.bpj.2014.09.011 [PubMed: 25418180]

97. Carzaniga R, Domart MC, Collinson LM, Duke E (2014) Cryo-soft x-ray tomography: A journey into the world of the native-state cell. Protoplasma. 251, 449–58. 10.1007/s00709-013-0583-y [PubMed: 24264466]

98. Cinquin BP, Do M, McDermott G, Walters AD, Myllys M, Smith EA, Cohen-Fix O, Le Gros MA, Larabell CA (2014) Putting molecules in their place. J Cell Biochem. 115, 209–16. 10.1002/jcb.24658 [PubMed: 23966233]

99. Young KD (2006) The selective value of bacterial shape. Microbiol Mol Biol Rev. 70, 660–703. 10.1128/MMBR.00001-06 [PubMed: 16959965]

100. Dove A (2016) Cell biology shapes up. Science. 354, 1052–4. 10.1126/science.354.6315.1055-d

101. Basiji DA, Ortyn WE, Liang L, Venkatachalam V, Morrissey P (2007) Cellular image analysis and imaging by flow cytometry. Clin Lab Med. 27, 653–70, viii. 10.1016/j.cll.2007.05.008 [PubMed: 17658411]

102. Hassell KL (2010) Population estimates of sickle cell disease in the u.S. Am J Prev Med. 38, S512–21. 10.1016/j.amepre.2009.12.022 [PubMed: 20331952]

103. Darrow MC, Zhang Y, Cinquin BP, Smith EA, Boudreau R, Rochat RH, Schmid MF, Xia Y, Larabell CA, Chiu W (2016) Visualizing red blood cell sickling and the effects of inhibition of sphingosine kinase 1 using soft x-ray tomography. J Cell Sci. 129, 3511–7. 10.1242/jcs.189225 [PubMed: 27505892]

104. Cole LW (2016) The evolution of per-cell organelle number. Front Cell Dev Biol. 4, 85 10.3389/fcell.2016.00085 [PubMed: 27588285]

105. Kowald A, Kirkwood TB (2011) Evolution of the mitochondrial fusion-fission cycle and its role in aging. Proc Natl Acad Sci U S A. 108, 10237–42. 10.1073/pnas.1101604108 [PubMed: 21646529]

106. Veltri KL, Espiritu M, Singh G (1990) Distinct genomic copy number in mitochondria of different mammalian organs. J Cell Physiol. 143, 160–4. 10.1002/jcp.1041430122 [PubMed: 2318903]

107. Yanagida M (2002) The model unicellular eukaryote, schizosaccharomyces pombe. Genome Biol. 3, COMMENT2003. 10.1186/gb-2002-3-3-comment2003

108. Parkinson DY, McDermott G, Etkin LD, Le Gros MA, Larabell CA (2008) Quantitative 3-d imaging of eukaryotic cells using soft x-ray tomography. J Struct Biol. 162, 380–6. 10.1016/j.jsb.2008.02.003 [PubMed: 18387313]

109. Gu W, Etkin LD, Le Gros MA, Larabell CA (2007) X-ray tomography of schizosaccharomyces pombe. Differentiation. 75, 529–35. 10.1111/j.1432-0436.2007.00180.x [PubMed: 17459084]
110. Larabell CA, Le Gros MA (2004) X-ray tomography generates 3-d reconstructions of the yeast, saccharomyces cerevisiae, at 60-nm resolution. Mol Biol Cell. 15, 957–62. 10.1091/mbc.E03-07-0522 [PubMed: 14699066]
111. Walters AD, May CK, Dauster ES, Cinquin BP, Smith EA, Robellet X, D'Amours D, Larabell CA, Cohen-Fix O (2014) The yeast polo kinase cdc5 regulates the shape of the mitotic nucleus. Curr Biol. 24, 2861–7. 10.1016/j.cub.2014.10.029 [PubMed: 25454593]
112. Roth MS, Cokus SJ, Gallaher SD, Walter A, Lopez D, Ericksson E, Endelman B, Westcott D, Larabell CA, Merchant SS, Pellgrini M, Niyogi KK (2017) Chromosome-level genome assembly and transcriptome of the green alga chromochloris zoefingiensis illuminates astaxanthin production. PNAS. In Press.
113. Hammel M, Amlanjyoti D, Reyes FE, Chen JH, Parpana R, Tang HY, Larabell CA, Tainer JA, Adhya S (2016) Hu multimerization shift controls nucleoid compaction. Sci Adv. 2, e1600650 10.1126/sciadv.1600650 [PubMed: 27482541]
114. McDermott G, Le Gros MA, Knoechel CG, Uchida M, Larabell CA (2009) Soft x-ray tomography and cryogenic light microscopy: The cool combination in cellular imaging. Trends Cell Biol. 19, 587–95. 10.1016/j.tcb.2009.08.005 [PubMed: 19818625]
115. Clowney EJ, LeGros MA, Mosley CP, Clowney FG, Markenskoff-Papadimitriou EC, Myllys M, Barnea G, Larabell CA, Lomvardas S (2012) Nuclear aggregation of olfactory receptor genes governs their monogenic expression. Cell. 151, 724–37. 10.1016/j.cell.2012.09.043 [PubMed: 23141535]
116. Clowney EJ, Lomvardas S, Larabell C (2014) Organizing gene regulatory events. Mol Biol Cell. 25.
117. Le Gros MA, Clowney EJ, Magklara A, Yen A, Markenscoff-Papadimitriou E, Colquitt B, Myllys M, Kellis M, Lomvardas S, Larabell CA (2016) Soft x-ray tomography reveals gradual chromatin compaction and reorganization during neurogenesis in vivo. Cell Rep. 17, 2125–36. 10.1016/j.celrep.2016.10.060 [PubMed: 27851973]
118. Ugarte F, Sousae R, Cinquin B, Martin EW, Krietsch J, Sanchez G, Inman M, Tsang H, Warr M, Passegue E, Larabell CA, Forsberg EC (2015) Progressive chromatin condensation and h3k9 methylation regulate the differentiation of embryonic and hematopoietic stem cells. Stem Cell Reports. 5, 728–40. 10.1016/j.stemcr.2015.09.009 [PubMed: 26489895]
119. Magowan C, Brown JT, Liang J, Heck J, Coppel RL, Mohandas N, Meyer-Ilse W (1997) Intracellular structures of normal and aberrant plasmodium falciparum malaria parasites imaged by soft x-ray microscopy. Proc Natl Acad Sci U S A. 94, 6222–7. [PubMed: 9177198]
120. Hanssen E, Knoechel C, Dearnley M, Dixon MW, Le Gros M, Larabell C, Tilley L (2012) Soft x-ray microscopy analysis of cell volume and hemoglobin content in erythrocytes infected with asexual and sexual stages of plasmodium falciparum. J Struct Biol. 177, 224–32. 10.1016/j.jsb.2011.09.003 [PubMed: 21945653]
121. Hanssen E, Knoechel C, Klonis N, Abu-Bakar N, Deed S, Legros M, Larabell C, Tilley L (2011) Cryo transmission x-ray imaging of the malaria parasite, p. Falciparum. J Struct Biol. 173, 161–8. [PubMed: 20826218]
122. Williams GJ, Hanssen E, Peele AG, Pfeifer MA, Clark J, Abbey B, Cadenazzi G, de Jonge MD, Vogt S, Tilley L, Nugent KA (2008) High-resolution x-ray imaging of plasmodium falciparum-infected red blood cells. Cytometry A. 73, 949–57. 10.1002/cyto.a.20616 [PubMed: 18671251]
123. Kapishnikov S, Grolimund D, Schneider G, Pereiro E, McNally JG, Als-Nielsen J, Leiserowitz L (2017) Unraveling heme detoxification in the malaria parasite by in situ correlative x-ray fluorescence microscopy and soft x-ray tomography. Sci Rep. 7, 7610 10.1038/s41598-017-06650-w [PubMed: 28790371]
124. Kapishnikov S, Leiserowitz L, Yang Y, Cloetens P, Pereiro E, Awamu Ndonglack F, Matuschewski K, Als-Nielsen J (2017) Biochemistry of malaria parasite infected red blood cells by x-ray microscopy. Sci Rep. 7, 802 10.1038/s41598-017-00921-2 [PubMed: 28400621]

125. Chichon FJ, Rodriguez MJ, Pereiro E, Chiappi M, Perdiguero B, Guttmann P, Werner S, Rehbein S, Schneider G, Esteban M, Carrascosa JL (2012) Cryo x-ray nano-tomography of vaccinia virus infected cells. J Struct Biol. 177, 202–11. Doi 10.1016/J.Jsb.2011.12.001 [PubMed: 22178221]

126. Aho V, Myllys M, Ruokolainen V, Hakanen S, Mantyla E, Virtanen J, Hukkanen V, Kuhn T, Timonen J, Mattila K, Larabell CA, Vihinen-Ranta M (2017) Chromatin organization regulates viral egress dynamics. Sci Rep. 7, 3692 10.1038/s41598-017-03630-y [PubMed: 28623258]

127. Myllys M, Ruokolainen V, Aho V, Smith EA, Hakanen S, Peri P, Salvetti A, Timonen J, Hukkanen V, Larabell CA, Vihinen-Ranta M (2016) Herpes simplex virus 1 induces egress channels through marginalized host chromatin. Sci Rep. 6, 28844 10.1038/srep28844 [PubMed: 27349677]

128. Morikawa T, Takubo K (2017) Use of imaging techniques to illuminate dynamics of hematopoietic stem cells and their niches. Front Cell Dev Biol. 5, 62 10.3389/fcell.2017.00062 [PubMed: 28660186]

129. Behzadi S, Serpooshan V, Tao W, Hamaly MA, Alkawareek MY, Dreaden EC, Brown D, Alkilany AM, Farokhzad OC, Mahmoudi M (2017) Cellular uptake of nanoparticles: Journey inside the cell. Chem Soc Rev. 46, 4218–44. 10.1039/c6cs00636a [PubMed: 28585944]

130. Chiappi M, Conesa JJ, Pereiro E, Sorzano CO, Rodriguez MJ, Henzler K, Schneider G, Chichon FJ, Carrascosa JL (2016) Cryo-soft x-ray tomography as a quantitative three-dimensional tool to model nanoparticle:Cell interaction. J Nanobiotechnology. 14, 15 10.1186/s12951-016-0170-4 [PubMed: 26939942]

131. Graf C, Meinke M, Gao Q, Hadam S, Raabe J, Sterry W, Blume-Peytavi U, Lademann J, Ruhl E, Vogt A (2009) Qualitative detection of single submicron and nanoparticles in human skin by scanning transmission x-ray microscopy. J Biomed Opt. 14, 021015 10.1117/1.3078811 [PubMed: 19405728]

132. Graf C, Nordmeyer D, Ahlberg S, Raabe J, Vogt A, Lademann J, Rancan F, Rühl E, editors. Penetration of spherical and rod-like gold nanoparticles into intact and barrier-disrupted human skin Colloidal Nanoparticles for Biomedical Applications X; 2015 2015/03/12/: SPIE.

133. Chiappi M, Conesa JJ, Pereiro E, Sorzano CO, Rodriguez MJ, Henzler K, Schneider G, Chichon FJ, Carrascosa JL (2016) Cryo-soft x-ray tomography as a quantitative three-dimensional tool to model nanoparticle:Cell interaction. J Nanobiotechnology. 14, 15 10.1186/s12951-016-0170-4 [PubMed: 26939942]

134. Jiang H, Song C, Chen CC, Xu R, Raines KS, Fahimian BP, Lu CH, Lee TK, Nakashima A, Urano J, Ishikawa T, Tamanoi F, Miao J (2010) Quantitative 3d imaging of whole, unstained cells by using x-ray diffraction microscopy. Proc Natl Acad Sci U S A. 107, 11234–9. 10.1073/pnas.1000156107 [PubMed: 20534442]

135. Krenkel M, Markus A, Bartels M, Dullin C, Alves F, Salditt T (2015) Phase-contrast zoom tomography reveals precise locations of macrophages in mouse lungs. Sci Rep. 5, 9973 10.1038/srep09973 [PubMed: 25966338]

136. Helfen L, Xu F, Suhonen H, Urbanelli L, Cloetens P, Baumbach T (2013) Nano-laminography for three-dimensional high-resolution imaging of flat specimens. Journal of Instrumentation. 8, C05006–C. Artn C05006 10.1088/1748-0221/8/05/C05006

137. Mokso R, Schwyn DA, Walker SM, Doube M, Wicklein M, Muller T, Stampanoni M, Taylor GK, Krapp HG (2015) Four-dimensional in vivo x-ray microscopy with projection-guided gating. Sci Rep. 5, 8727 10.1038/srep08727 [PubMed: 25762080]

138. dos Santos Rolo T, Ershov A, van de Kamp T, Baumbach T (2014) In vivo x-ray cine-tomography for tracking morphological dynamics. Proc Natl Acad Sci U S A. 111, 3921–6. 10.1073/pnas.1308650111 [PubMed: 24594600]

139. Moosmann J, Ershov A, Altapova V, Baumbach T, Prasad MS, LaBonne C, Xiao X, Kashef J, Hofmann R (2013) X-ray phase-contrast in vivo microtomography probes new aspects of xenopus gastrulation. Nature. 497, 374–7. 10.1038/nature12116 [PubMed: 23676755]

140. Moosmann J, Ershov A, Weinhardt V, Baumbach T, Prasad MS, LaBonne C, Xiao X, Kashef J, Hofmann R (2014) Time-lapse x-ray phase-contrast microtomography for in vivo imaging and analysis of morphogenesis. Nat Protoc. 9, 294–304. 10.1038/nprot.2014.033 [PubMed: 24407356]

141. Lowe T, Garwood RJ, Simonsen TJ, Bradley RS, Withers PJ (2013) Metamorphosis revealed: Time-lapse three-dimensional imaging inside a living chrysalis. J R Soc Interface. 10, 20130304 10.1098/rsif.2013.0304 [PubMed: 23676900]

142. Xu F, Helfen L, Suhonen H, Elgrabli D, Bayat S, Reischig P, Baumbach T, Cloetens P (2012) Correlative nanoscale 3d imaging of structure and composition in extended objects. PLoS One. 7, e50124 10.1371/journal.pone.0050124 [PubMed: 23185554]

143. Deng J, Vine DJ, Chen S, Jin Q, Nashed YS, Peterka T, Vogt S, Jacobsen C (2017) X-ray ptychographic and fluorescence microscopy of frozen-hydrated cells using continuous scanning. Sci Rep. 7, 445 10.1038/s41598-017-00569-y [PubMed: 28348401]

144. Cagno S, Brede DA, Nuyts G, Vanmeert F, Pacureanu A, Tucoulou R, Cloetens P, Falkenberg G, Janssens K, Salbu B, Lind OC (2017) Combined computed nanotomography and nanoscopic x-ray fluorescence imaging of cobalt nanoparticles in caenorhabditis elegans. Anal Chem. 89, 11435–42. 10.1021/acs.analchem.7b02554 [PubMed: 28994576]

145. Barrea RA, Gore D, Kujala N, Karanfil C, Kozyrenko S, Heurich R, Vukonich M, Huang R, Paunesku T, Woloschak G, Irving TC (2010) Fast-scanning high-flux microprobe for biological x-ray fluorescence microscopy and microxas. J Synchrotron Radiat. 17, 522–9. 10.1107/S0909049510016869 [PubMed: 20567085]

146. Combs CA Fluorescence microscopy: A concise guide to current imaging methods Current protocols in neuroscience: John Wiley & Sons, Inc.; 2010.

147. Smith EA, Cinquin BP, McDermott G, Le Gros MA, Parkinson DY, Kim HT, Larabell CA (2013) Correlative microscopy methods that maximize specimen fidelity and data completeness, and improve molecular localization capabilities. J Struct Biol. 184, 12–20. 10.1016/j.jsb.2013.03.006 [PubMed: 23531637]

148. Smith EA, Cinquin BP, McDermott G, Le Gros MA, Larabell CA Correlated soft x-ray tomography and cryo-light microscopy In: Howard GC, Brown WE, Auer M, editors. Imaging life: Biological systems from atoms to tissues. USA: Oxford University Press; 2014.

149. Ekman AA, Chen JH, Guo J, McDermott G, Le Gros MA, Larabell CA (2017) Mesoscale imaging with cryo-light and x-rays: Larger than molecular machines, smaller than a cell. Biol Cell. 109, 24–38. 10.1111/boc.201600044 [PubMed: 27690365]

150. Cinquin BP, Do M, McDermott G, Walters AD, Myllys M, Smith EA, Cohen-Fix O, Le Gros MA, Larabell CA (2014) Putting molecules in their place. J Cell Biochem. 115, 209–16. 10.1002/jcb.24658 [PubMed: 23966233]

151. Hagen C, Werner S, Carregal-Romero S, A NM, B GK, Guttmann P, Rehbein S, Henzler K, T CM, D JV, W JP, Schneider G, Grunewald K (2014) Multimodal nanoparticles as alignment and correlation markers in fluorescence/soft x-ray cryo-microscopy/tomography of nucleoplasmic reticulum and apoptosis in mammalian cells. Ultramicroscopy. 146C, 46–54. 10.1016/j.ultramic.2014.05.009

152. Hagen C, Guttmann P, Klupp B, Werner S, Rehbein S, Mettenleiter TC, Schneider G, Grunewald K (2012) Correlative vis-fluorescence and soft x-ray cryo-microscopy/tomography of adherent cells. J Struct Biol. 177, 193–201. Doi 10.1016/J.Jsb.2011.12.012 [PubMed: 22210307]

153. Chen HY, Chiang DM, Lin ZJ, Hsieh CC, Yin GC, Weng IC, Guttmann P, Werner S, Henzler K, Schneider G, Lai LJ, Liu FT (2016) Nanoimaging granule dynamics and subcellular structures in activated mast cells using soft x-ray tomography. Sci Rep. 6, 34879 10.1038/srep34879 [PubMed: 27748356]

154. Elgass KD, Smith EA, LeGros MA, Larabell CA, Ryan MT (2015) Analysis of er-mitochondria contacts using correlative fluorescence microscopy and soft x-ray tomography of mammalian cells. J Cell Sci. 128, 2795–804. 10.1242/jcs.169136 [PubMed: 26101352]

155. Tsien RY (1981) A non-disruptive technique for loading calcium buffers and indicators into cells. Nature. 290, 527–8. DOI 10.1038/290527a0 [PubMed: 7219539]

156. Tsien RY (1980) New calcium indicators and buffers with high selectivity against magnesium and protons: Design, synthesis, and properties of prototype structures. Biochemistry. 19, 2396–404. 10.1021/bi00552a018 [PubMed: 6770893]

157. Fields RD, Burnstock G (2006) Purinergic signalling in neuron-glia interactions. Nat Rev Neurosci. 7, 423–36. 10.1038/nrn1928 [PubMed: 16715052]

158. Grienberger C, Konnerth A (2012) Imaging calcium in neurons. Neuron. 73, 862–85. 10.1016/j.neuron.2012.02.011 [PubMed: 22405199]

159. Krishna SS, Majumdar I, Grishin NV (2003) Structural classification of zinc fingers: Survey and summary. Nucleic Acids Res. 31, 532–50. 10.1093/nar/gkg161 [PubMed: 12527760]

160. Gamsjaeger R, Liew CK, Loughlin FE, Crossley M, Mackay JP (2007) Sticky fingers: Zinc-fingers as protein-recognition motifs. Trends Biochem Sci. 32, 63–70. 10.1016/j.tibs.2006.12.007 [PubMed: 17210253]

161. Lindh U (1995) Cell biology, trace-elements and nuclear microscopy. Nuclear Instruments & Methods in Physics Research Section B-Beam Interactions with Materials and Atoms. 104, 285–91. Doi 10.1016/0168-583x(95)00389-4

162. McRae R, Bagchi P, Sumalekshmy S, Fahrni CJ (2009) In situ imaging of metals in cells and tissues. Chem Rev. 109, 4780–827. 10.1021/cr900223a [PubMed: 19772288]

163. Karunakaran C, Christensen CR, Gaillard C, Lahlali R, Blair LM, Perumal V, Miller SS, Hitchcock AP (2015) Introduction of soft x-ray spectromicroscopy as an advanced technique for plant biopolymers research. PLoS One. 10, e0122959 10.1371/journal.pone.0122959 [PubMed: 25811457]

164. Thieme J, McNult I, Vogt S, Paterson a.D. (2007) X-ray spectromicroscopy—a tool for environmental sciences. Environ Sci Technol. 41, 6885–9. 10.1021/es0726254 [PubMed: 17993124]

165. Sviben S, Gal A, Hood MA, Bertinetti L, Politi Y, Bennet M, Krishnamoorthy P, Schertel A, Wirth R, Sorrentino A, Pereiro E, Faivre D, Scheffel A (2016) A vacuole-like compartment concentrates a disordered calcium phase in a key coccolithophorid alga. Nat Commun. 7, 11228 10.1038/ncomms11228 [PubMed: 27075521]

166. Kim AM, Vogt S, O'Halloran TV, Woodruff TK (2010) Zinc availability regulates exit from meiosis in maturing mammalian oocytes. Nat Chem Biol. 6, 674–81. 10.1038/nchembio.419 [PubMed: 20693991]

167. Telling ND, Everett J, Collingwood JF, Dobson J, van der Laan G, Gallagher JJ, Wang J, Hitchcock AP (2017) Iron biochemistry is correlated with amyloid plaque morphology in an established mouse model of alzheimer's disease. Cell Chem Biol. 24, 1205–15 e3. 10.1016/j.chembiol.2017.07.014 [PubMed: 28890316]

168. Takamiya M, Xu F, Suhonen H, Gourain V, Yang L, Ho NY, Helfen L, Schrock A, Etard C, Grabher C, Rastegar S, Schlunck G, Reinhard T, Baumbach T, Strahle U (2016) Melanosomes in pigmented epithelia maintain eye lens transparency during zebrafish embryonic development. Sci Rep. 6, 25046 10.1038/srep25046 [PubMed: 27141993]

169. James SA, Hare DJ, Jenkins NL, de Jonge MD, Bush AI, McColl G (2016) Erratum: Phixanes: In vivo imaging of metal-protein coordination environments. Sci Rep. 6, 22684 10.1038/srep22684 [PubMed: 26998588]

170. Obst M, Schmid G (2014) 3d chemical mapping: Application of scanning transmission (soft) x-ray microscopy (stxm) in combination with angle-scan tomography in bio-, geo-, and environmental sciences. Methods Mol Biol. 1117, 757–81. 10.1007/978-1-62703-776-1_34 [PubMed: 24357389]

171. Singla J, McClary KM, White KL, Alber F, Sali A, Stevens RC (2018) Opportunities and challenges in building a spatiotemporal multi-scale model of the human pancreatic beta cell. Cell. 173, 11–9. 10.1016/j.cell.2018.03.014 [PubMed: 29570991]

172. Prewitt JMS, Mendelsohn ML (2006) The analysis of cell images*. Ann N Y Acad Sci. 128, 1035–53. 10.1111/j.1749-6632.1965.tb11715.x

173. Fogelqvist E, Kordel M, Carannante V, Onfelt B, Hertz HM (2017) Laboratory cryo x-ray microscopy for 3d cell imaging. Sci Rep. 7, 13433 10.1038/s41598-017-13538-2 [PubMed: 29044158]

174. Lovric G, Vogiatzis Oikonomidis I, Mokso R, Stampanoni M, Roth-Kleiner M, Schittny JC (2017) Automated computer-assisted quantitative analysis of intact murine lungs at the alveolar scale. PLoS One. 12, e0183979 10.1371/journal.pone.0183979 [PubMed: 28934236]

175. Vogelgesang M, Chilingaryan S, Rolo T.d.S., Kopmann A, editors. Ufo: A scalable gpu-based image processing framework for on-line monitoring. 2012 IEEE 14th International Conference

on High Performance Computing and Communication & 2012 IEEE 9th International Conference on Embedded Software and Systems; 2012 2012/06//: IEEE.

176. Cardenes R, Zhang C, Klementieva O, Werner S, Guttmann P, Pratsch C, Cladera J, Bijnens BH (2017) 3d membrane segmentation and quantification of intact thick cells using cryo soft x-ray transmission microscopy: A pilot study. PLoS One. 12, e0174324 10.1371/journal.pone.0174324 [PubMed: 28376110]

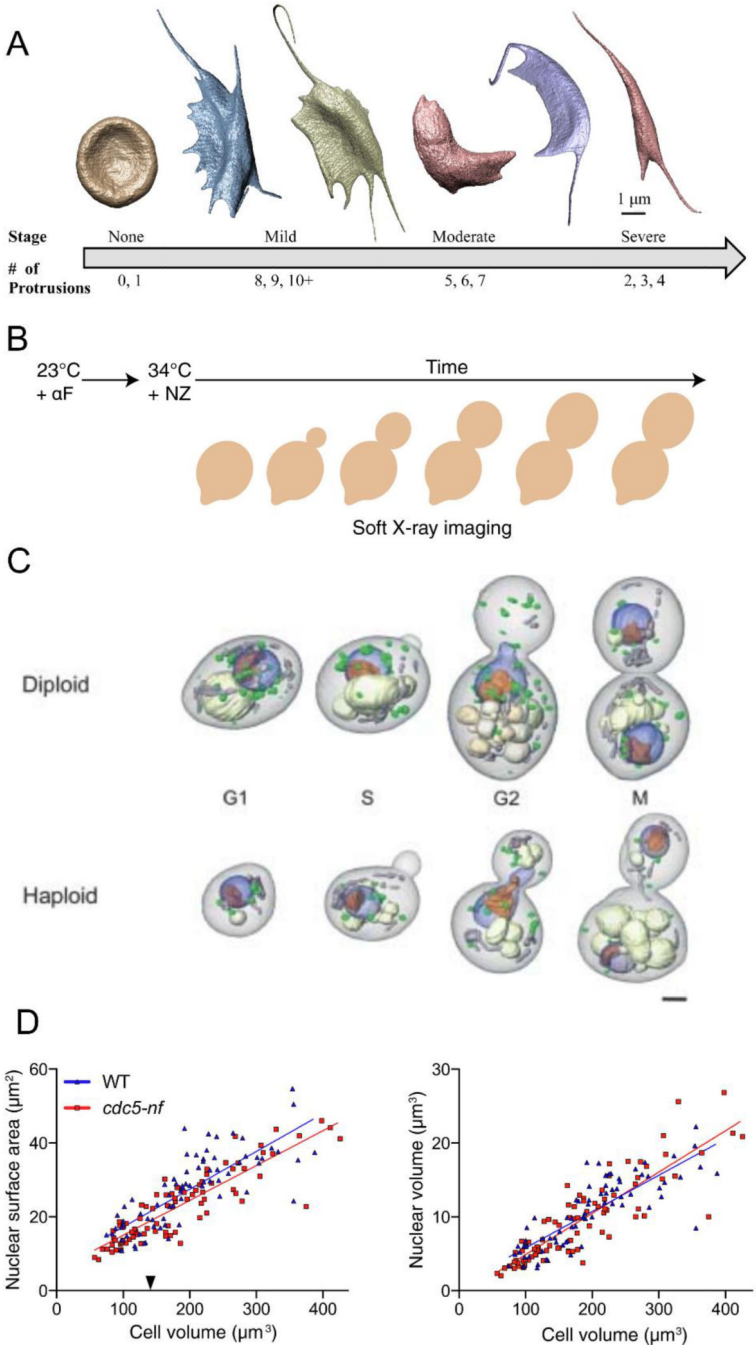

Figure 1.

A. Morphological study of the four stages of sickle cell anemia in red blood cells carried out by Soft X-ray tomography [103].

B. Diagrammatic representation of cell division in the yeast *S. cerevisiae* [111], NZ - nocodazole.

C. Soft X-ray tomographic study showing the internal morphological changes that takes place during *S. cerevisiae* cell division. Scale bar = 2 µm [77].

D. Example of quantitative morphological information obtained using soft X-ray tomography. Quantification of nuclear surface areas as a function of cell size of wild type (WT) and mutated (cdc5-nf) cells. This mutation results in ‘nuclear flares’ that appear in cells with a volume of 140 μm^3 (black triangle, left hand plot). The plot on the right quantifies nuclear volume as a function of cell size, showing there is no difference in this ratio between wild-type and mutant cells [111].

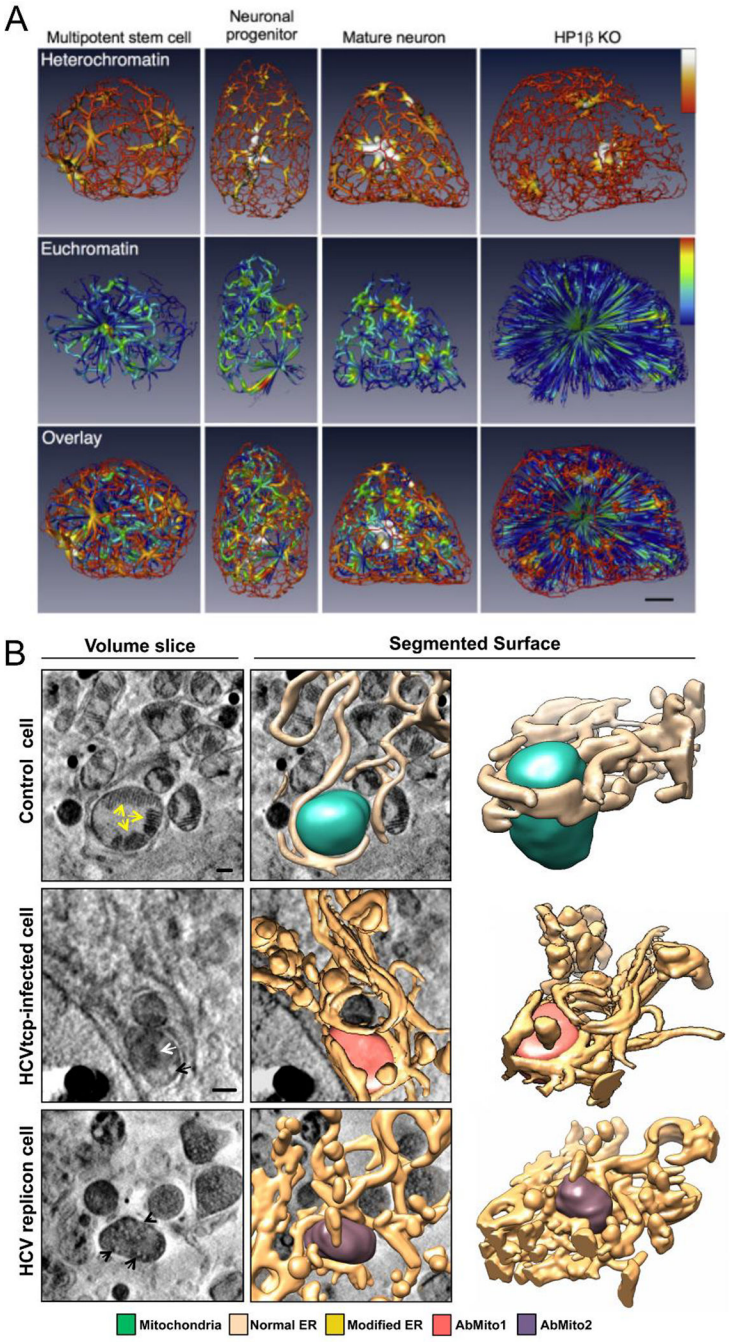

Figure 2.

A. Soft X-ray analysis of chromatin masses in the nuclei of three types of olfactory epithelium cells, namely multipotent stem cells, neuronal progenitors, and terminally differentiated neurons, together with similar data from HP1β knockout (KO) cells [117]. This morphological study revealed a surprising degree of connectivity exists between chromatin and this persists throughout development and differentiation. Scale bar = 2 μm. B. Alteration of the endoplasmic reticulum-mitochondria interface in Hepatitis C virus (HCV) replicating cells [78]. Comparative analysis of the endoplasmic reticulum-

mitochondria topological relationship of vitrified control (A), HCVtcp-infected (B), or HCV replicon-bearing cells (C). Volumes slices, manually segmented surface representation, and surface views of the different areas of interest are shown. Yellow arrows in (A) mark mitochondrial cristae. Two types of abnormal mitochondria were found class 1 (AbMito1) and class 2 (AbMito2). White and black arrows mark matrix condensation arrows and cristae swelling, respectively. Scale bars 0.5 μm.

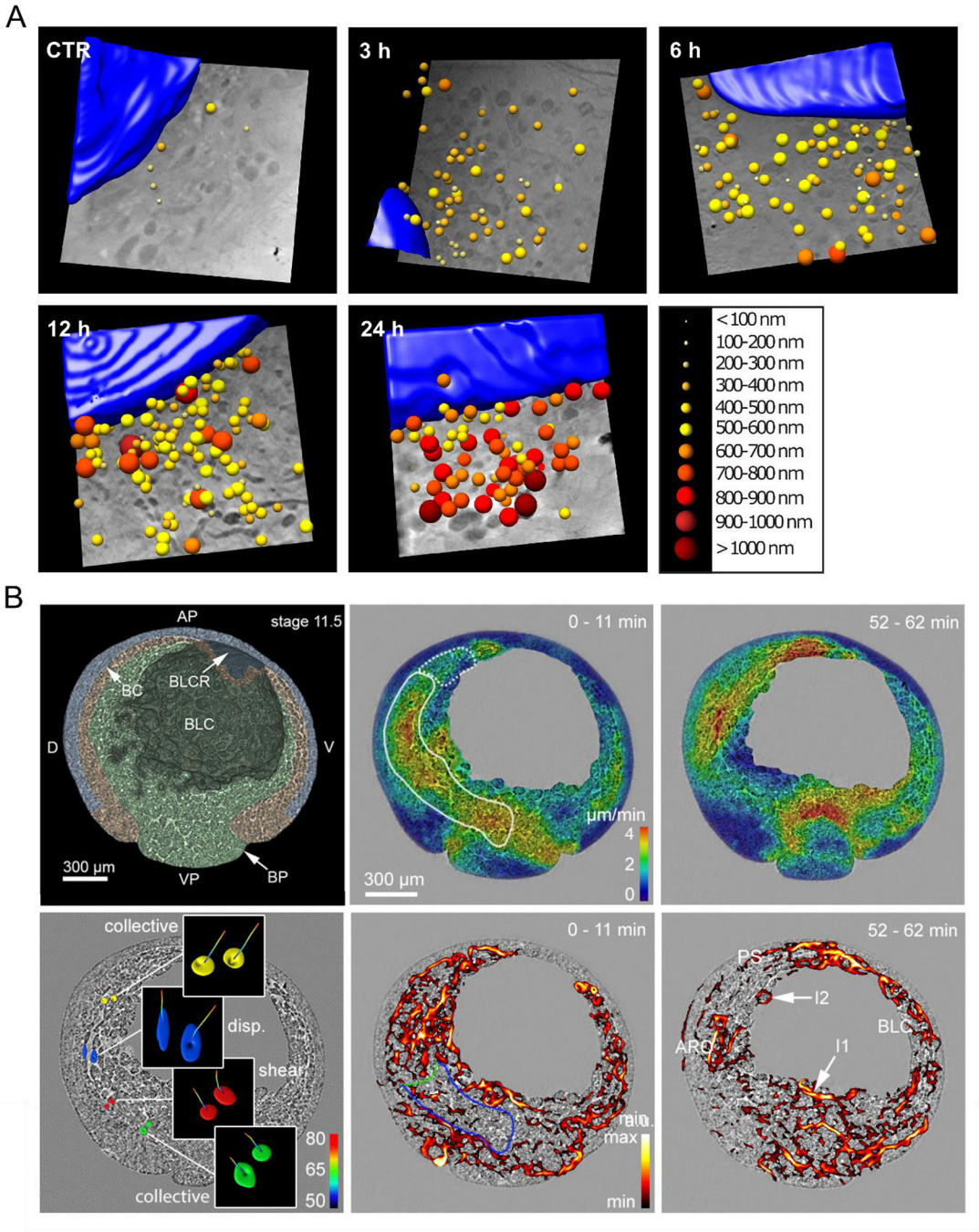

Figure 3.

A. Soft X-ray tomographic analysis of endosome size in breast cancer (MCF-7) cells incubated with superparamagnetic iron oxide nanoparticles (SPION) for 0 (CTR), 3, 6, 12 and 24 h [133]. The nucleus is shown in blue. Field of view, 11.5 µm x 11.5 µm. SPIONs are color-coded according to size.

B. 3D time-lapse cell tracking during gastrulation of African frog *Xenopus laevis [139].* Virtual cut through 3D embryo rendering at stage 11.5 depicting ectoderm (blue), mesoderm (orange) and endoderm (green). Abbreviations: dorsal (D), ventral (V), animal pole (AP),

vegetal pole (VP), blastocoel (BLC), Brachet's cleft (BC), blastocoel roof (BLCR). Magnitude of velocity on sagittal slice for two different times. 3D rendering of the highlighted cell pairs in the archenteron and associated trajectories over period of 30min. 3D Velocity field showing difference in collective and singular cell motion at two various times.

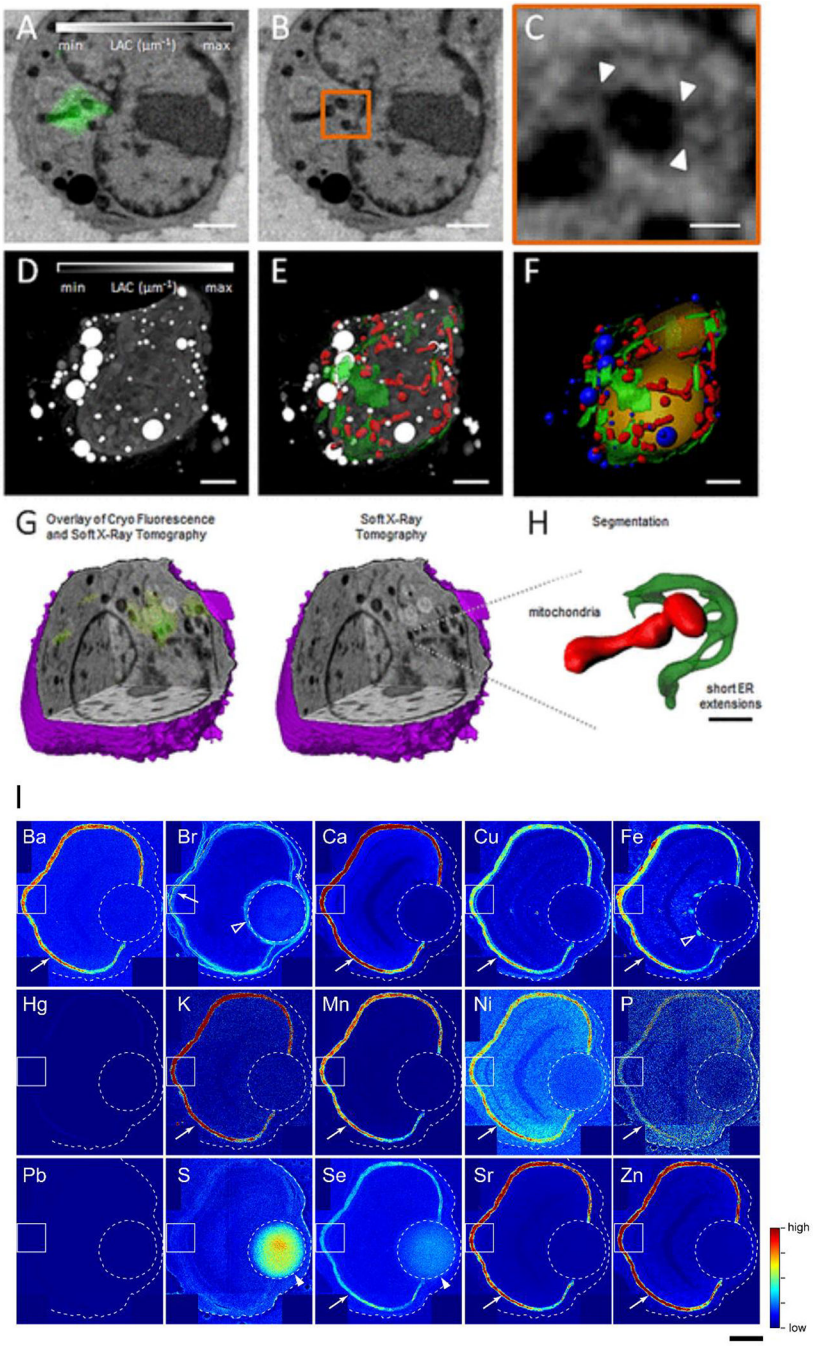

Figure 4.

A. Two-dimensional computer-generated section (typically known as an orthoslice) from a reconstruction of a mouse lymphoblastoid cell expressing MiD51–GFP (green), generated using correlated cryo-fluorescence tomography and soft X-ray tomography [154].

B. The same computer-generated slice from the SXT reconstruction as presented in A without fluorescence overlay. The orange rectangle outlines the area of concentrated MiD51–GFP fluorescence.

C. Magnification of the area shown in A and B containing a concentration of MiD51–GFP. White arrowheads indicate positions of ER–mitochondria contact sites.
D. Maximum intensity projection of the full 3D SXT reconstruction with the contrast reversed so that features that are low-absorbing are shaded black and features that are highly absorbent are shaded white.
E. ER (green) and mitochondria (red) segmented out and overlaid with the reconstruction.
F. Surface rendering of segmented cellular features, including the nucleus (orange), lipid droplets (blue), ER (green) and mitochondria (red).
G. Three-dimensional cutaway of the SXT-generated reconstruction reveals the same 3D location of the MiD51–GFP fluorescence of that shown in A.
H. Detailed view of small ER extensions contacting the mitochondria at the MiD51 foci. Scale bars: 2 μm (A, B, D–F); 400 nm (C); 1 μm (H).
I. Localization of elements in the different tissues of the eye, such as lens fiber and retinal pigment epithelium, of a 3-dpf (days post fertilization) zebrafish embryo [168].

Table 1.

List of known and commonly used X-ray microscope methods to study morphology and physiology via trace elements of cells. Contrast, resolution, penetration depth and time required for full acquisition are average values of what has been used in the past for cell biology.

Morphology (transmission)				
Method	**Contrast modality**	**Resolution (nm)**	**Penetration depth, (μm)**	**Time required for one tomogram, (mins)**
Soft x-ray microscopy (43,58)	“Water window” absorption edges of C, O, & N	25	10	5
Soft x-ray coherent diffraction imaging (40, 42, 52)	Phase-contrast	25	20	50
Hard x-ray microscopy (44–46)	Chemical staining Zernike-like phase contrast	30	60	30
Hard x-ray projection tomography (55–57)	Phase contrast	50	1000	5
Physiology (scanning)				
Soft scanning fluorescence microscope (136,144)	C, N, O, P, & S	25	-	80
Hard scanning fluorescence microscopy (119, 142)	Ca, Fe, Co, & Zn	50	-	180